

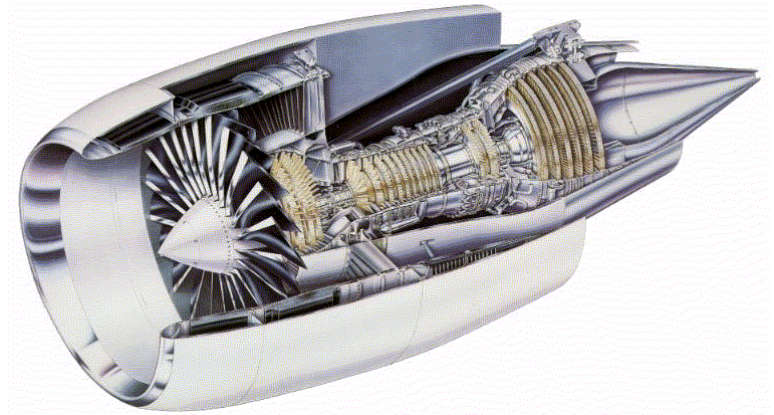
Structure and Mechanical Properties of Oxidation Resistant Alloys

Kevin Hemker

Johns Hopkins

hemker@jhu.edu





*"The development of ever more efficient gas turbines has always been paced by the results of research and development in the concurrent fields of **design** and **materials technology**."*

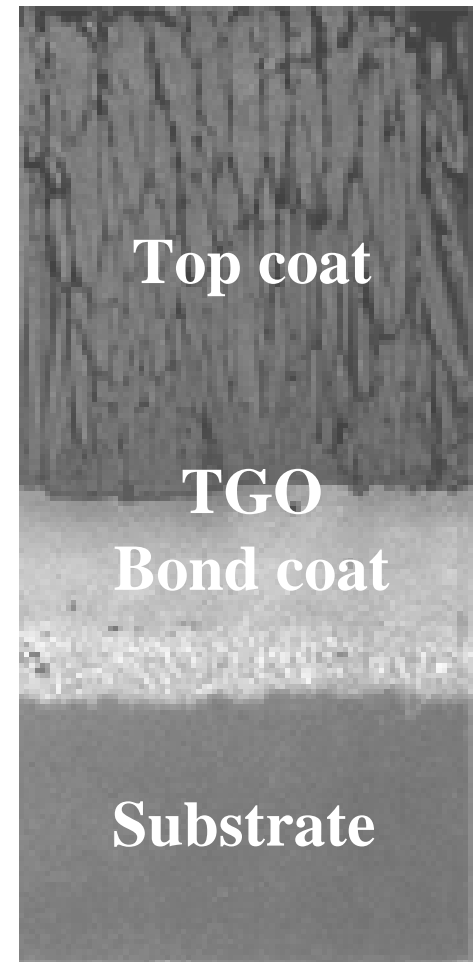
- G.W Goward

Surface and Coatings Tech, 108-109 (1998) 73-79

"Improved structural design and cooling technology applied to higher strength-at-temperature alloys cast by increasingly complex methods, and coated with steadily improved coating systems, have lead to remarkably efficient turbine engines."

- G.W Goward

Surface and Coatings Tech, 108-109 (1998) 73-79



A modern TBS

Drivers for bond coat design

- Improve oxidation resistance and slow TGO formation.
- Increase bond coat strength.
- Alloy to avoid phase transformations and CTE mismatch with substrate.

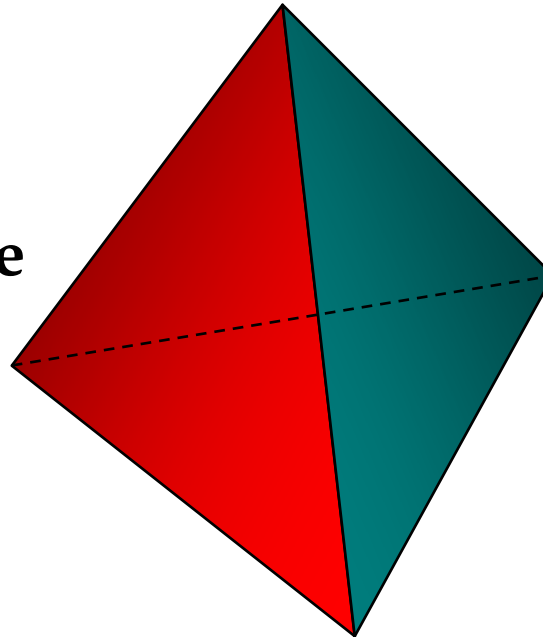
Paradigm for materials development

Performance

- *reduced weight*
- *increased temperature*

Microstructure

- *crystal structure*
- *grain size*
- *defects*
- *phases*



Processing

- *vapor deposition*
- *electrodeposition*
- *cast*
- *wrought*

Properties

- *modulus, strength, CTE*
- *temperature resistance*

Outline

- A brief history of oxidation resistant alloys and coatings
- Diffusion aluminide bond coats
 - Microstructure
 - Properties
 - Factors influencing ratcheting
- Overlay bond coats
 - Microstructure
 - Properties
 - Factors influencing delamination

Delhi Iron Pillar



- The famous iron pillar in Delhi is a metallurgical wonder. This huge wrought iron pillar, 24 feet in height 16.4 inches in diameter at the bottom, and 6 1/2 tons in weight has stood exposed to tropical sun and rain for 1,600 years without showing any visible signs of rusting or corrosion.
- High concentrations of P catalyze the formation of δ -FeOOH (iron oxyhydroxide), which is amorphous in nature and forms as an adherent compact layer next to the metal-scale interface, Upon formation, the corrosion resistance is significantly enhanced because δ -FeOOH forms a barrier between the rust and the metal."
- Balasubramaniam (IIT)

Paths to oxidation resistance

• Alloying

- With select oxide formers
- Self healing
- Requires considerable quantities of solute
- Must not degrade other properties (e.g. creep)

• Coatings

- Must be applied
- Must retard oxidation
- Must be adherent
- Cannot degrade properties of the substrate

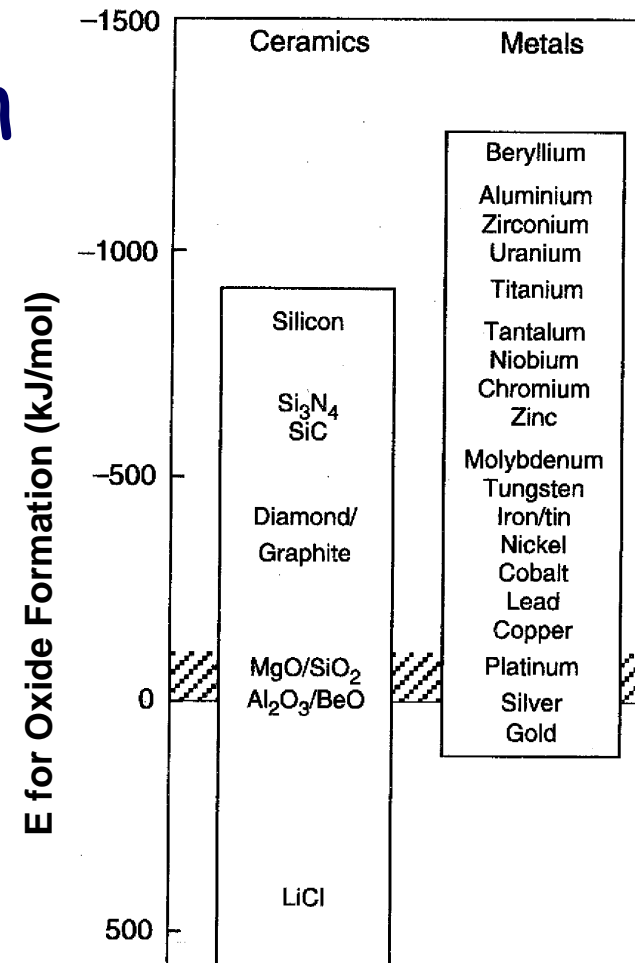
Select oxide formers

• Preferential oxidation

- Must form oxide or protective layer before base metal oxide is formed

• Protective

- Must form a dense, slow growing, protective film
- E.g. Cr_2O_3 , Al_2O_3 , SiO_2



Alloying of steels

• Low carbon steels

- Cheap, easily formed, and mechanically strong, but rust at low T and oxidizes at high T.

• Stainless steels

- Add significant quantities of Cr (~18%) which forms a very protective oxide film
- Cuts down the rate of attack by 100 times @ 900°C
- Affects microstructure and mechanical properties
- Other elements (e.g. Al, Si, P) also beneficial

Influence of Cr in superalloys

• Metal loss (a la Ashby)

- Ni → NiO
 - Ni loss ~0.1mm in 600h at $0.7T_m \sim 950^\circ\text{C}$
- Cr → Cr₂O₃
 - Cr loss ~0.1mm in 1600h at $0.7T_m \sim 1,231^\circ\text{C}$
 - Cr loss ~0.1mm in 1,000,000h at 950°C
- Ni20% Cr → Cr₂O₃
 - Ni20%Cr loss ~0.1mm in 6,000h at 950°C
 - Foreign elements increase diffusion rates
- Commercial superalloys limited to <10%Cr
 - Not sufficient to protect alloy from oxidation!

Alloying of Ni-base superalloys

- Modern superalloys have been engineered over decades and contain ~10 elements.

Composition of Single-crystalline René N5

Element:	<u>Ni</u>	<u>Co</u>	<u>Cr</u>	<u>Ta</u>	<u>Al</u>	<u>W</u>	<u>Re</u>	<u>Mo</u>	<u>Hf</u>	<u>Ti</u>	<u>C</u>
Wt%	63.38	7.33	7.03	6.42	6.05	5.13	3.05	1.40	0.15	0.01	0.05
At%	64.92	7.48	8.13	2.13	13.48	1.68	0.99	0.88	0.05	0.01	0.25

- The **composition** of most elements is **restricted** by processing windows and mechanical property requirements.

Diffusion aluminide coatings

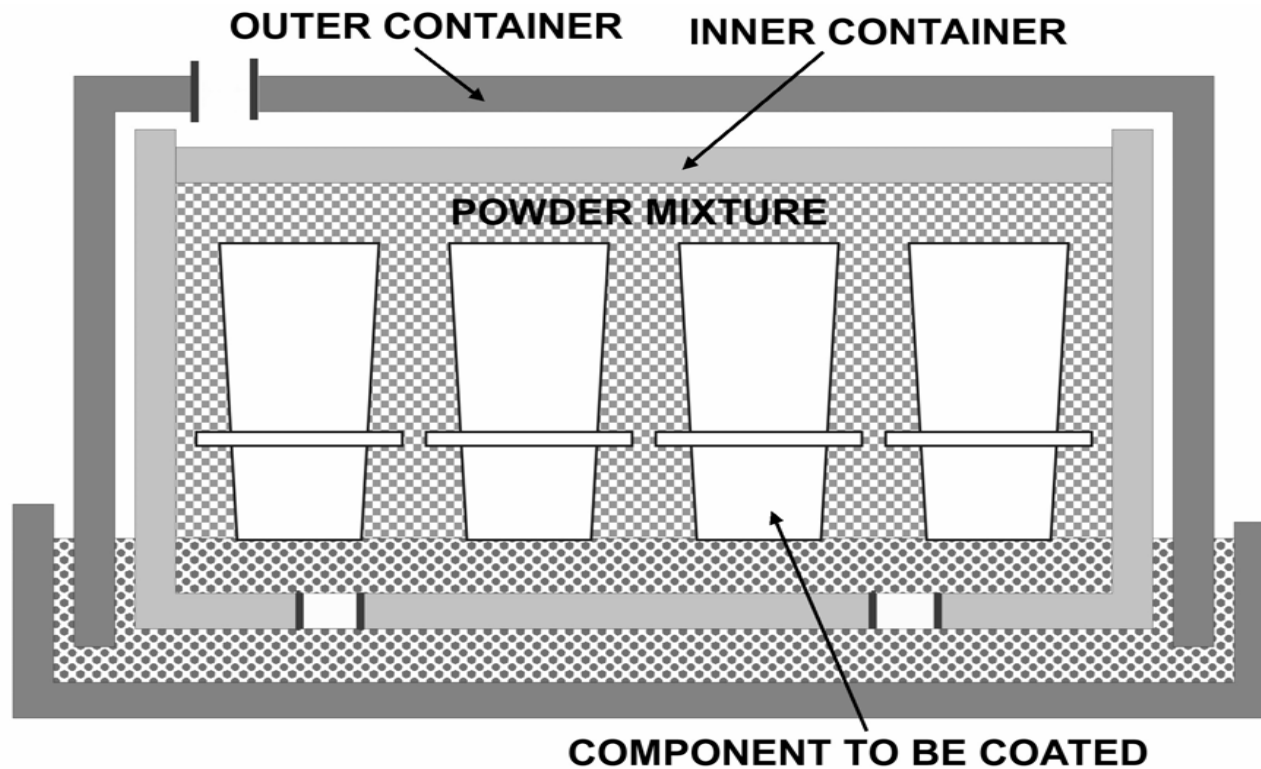
• Pack cementation aluminizing

- Parts packed in Al powder, sal ammoniac (NH_4Cl), graphite and alumina filler and heated to 450°C for 2h.
- First used for Fe wire or ribbon heating elements, Cu condenser tubes, etc.

• First patent

- Van Aller, Allison, Hawkins (GE) 1911
 - Way to 'calorize' metals to render them 'inoxidizable'
 - Attributed to selective formation of alumina scales

Schematic of the pack cementation process



Pack cementation reactions

Pack Components

Source (Cr, Al, Si or their alloys)

Activator (NaCl, NH₄Cl or other halide)

Inert Filler (often alumina)

Reactions between Source and Activator (Aluminizing)



Deposition on Substrate (Aluminizing)

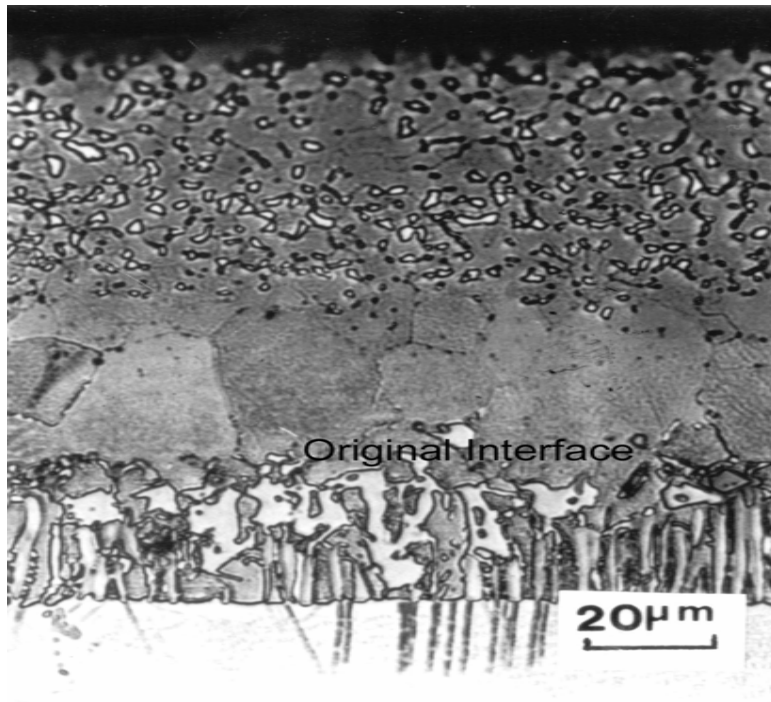


And, for activators which contain hydrogen e.g. NH₄Cl,

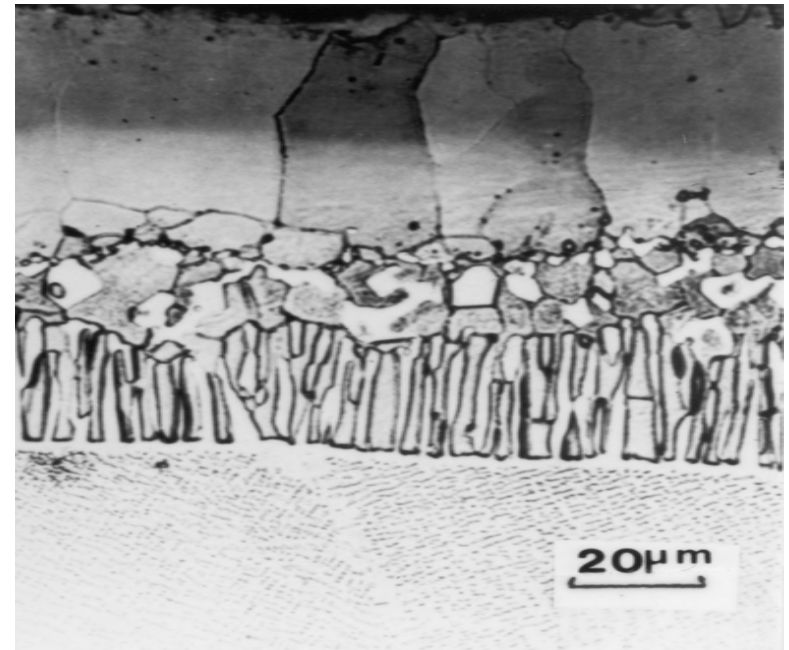


(The underlined symbols refer to species in the solid substrate.)

Pack cementation coatings

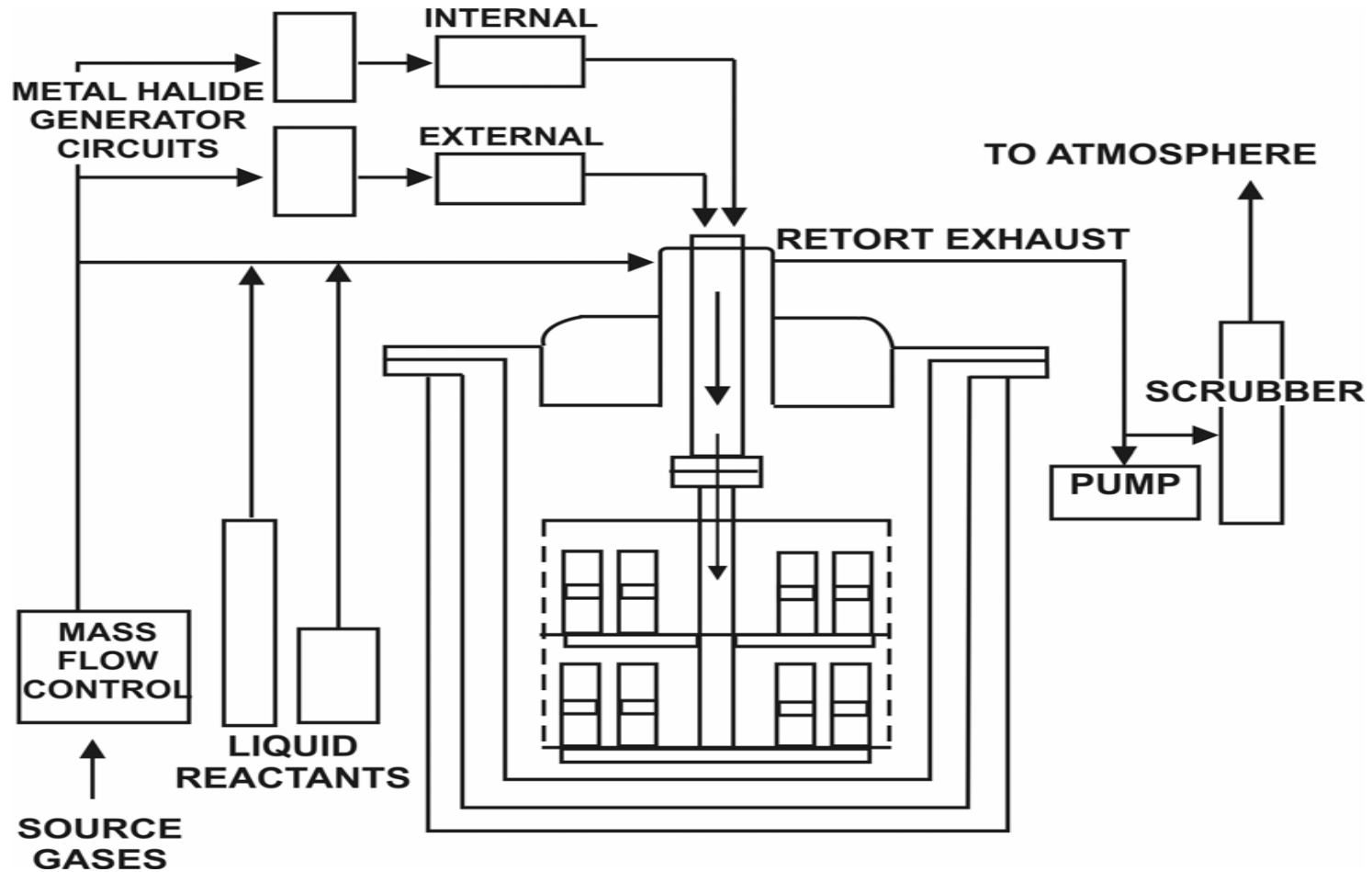


High-activity diffusion coating
on a Ni-base superalloy
- Al diffuses in -



Low-activity diffusion coating
on a Ni-base superalloy
- Ni diffuses out -

Schematic of CVD processing



Aero history of diffusion aluminides

• 1950's

- Allison and Curtiss Wright - hot dipping of Ni blades

• 1960's

- P&W - aluminizing of Ni blades by slurry processing

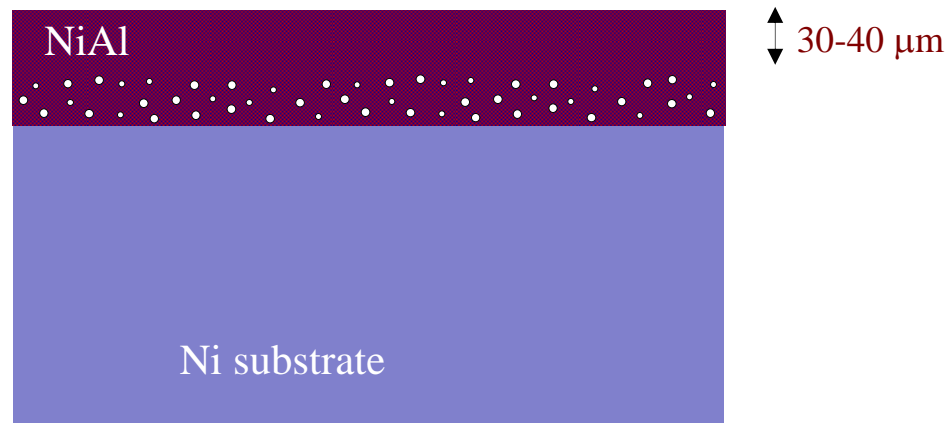
• 1970's

- Most vane and blade coatings applied by "pack cementation" and more recently by CVD

• 1990's

- Recognized as useful TBC bond coats
 - Forms an adherent $\alpha\text{-Al}_2\text{O}_3$ TGO

Making a diffusion aluminide coating

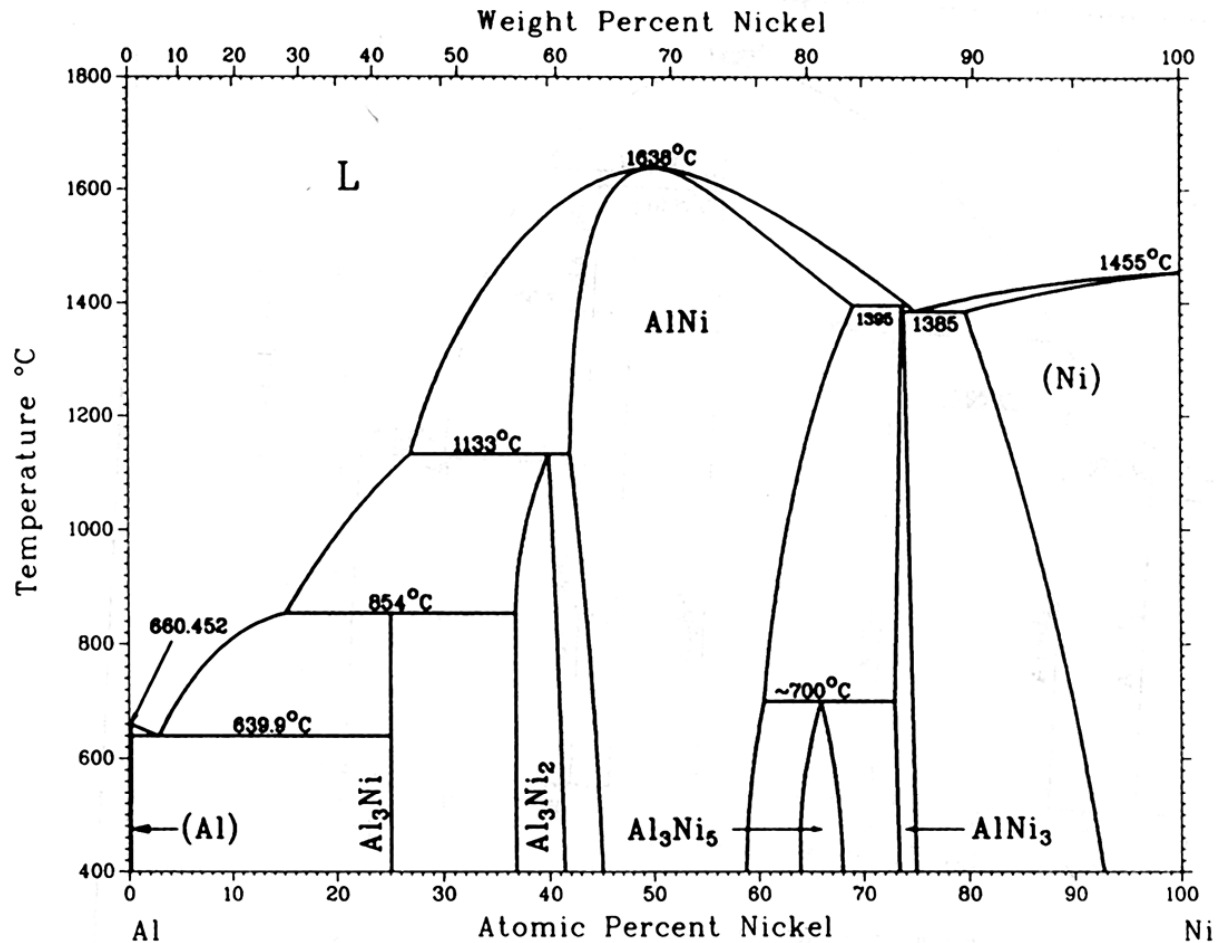


- Ni and Al diffuse together and form an **intermetallic** coating

Ni-Al binary phase diagram:



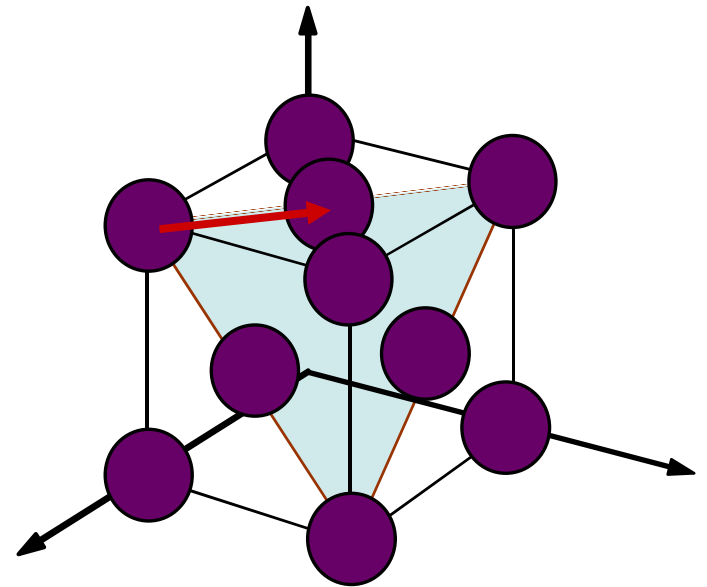
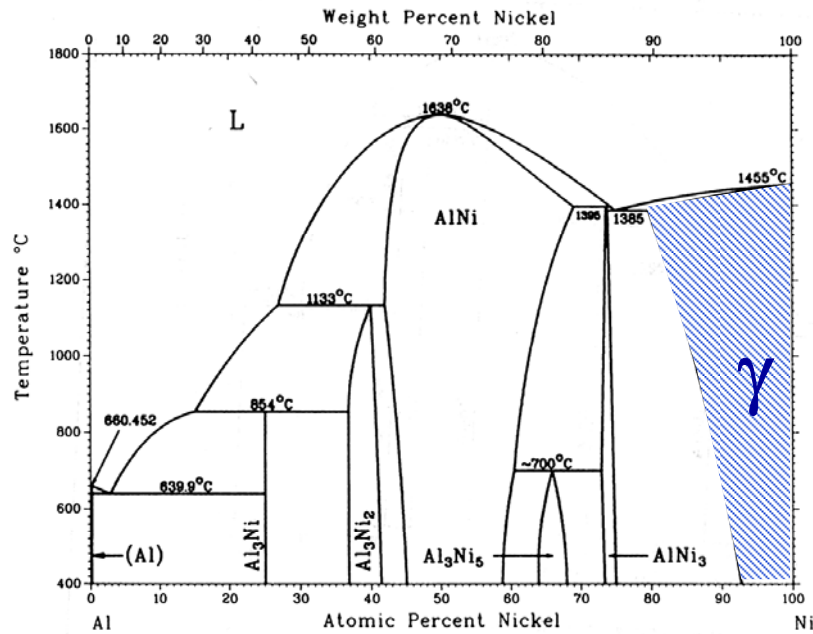
Al-Ni Phase Diagram



Ni-Al binary phase diagram:



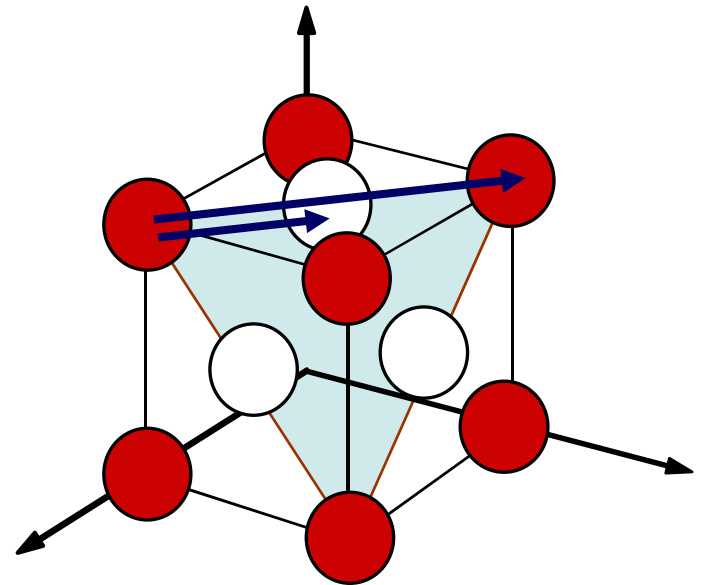
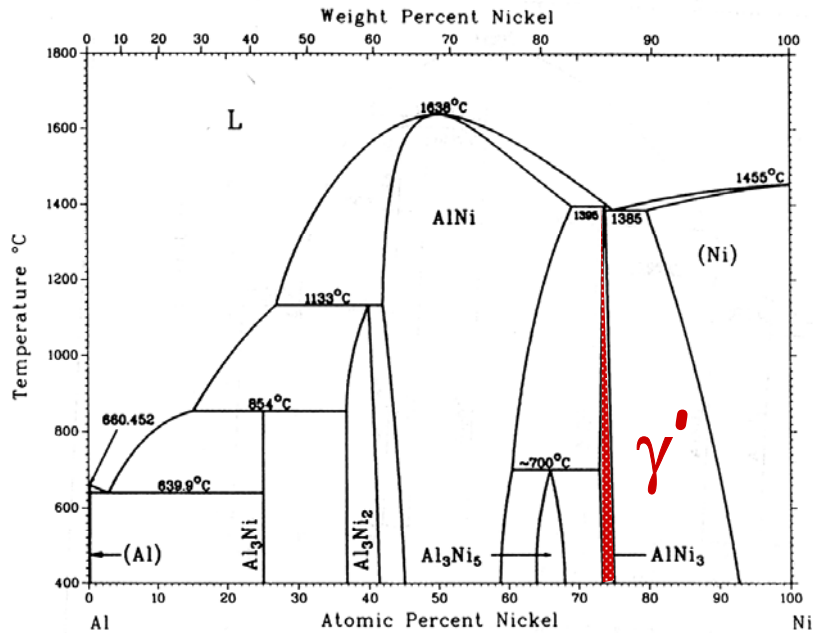
Al-Ni Phase Diagram



FCC

Ni-Al binary phase diagram:

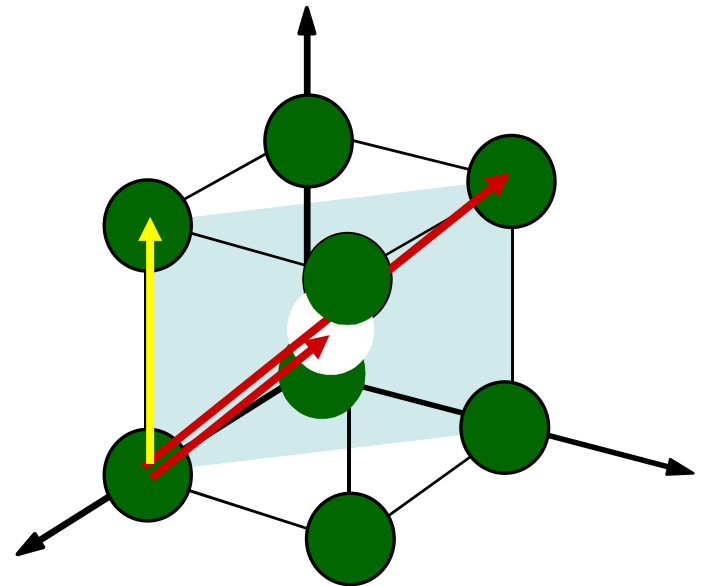
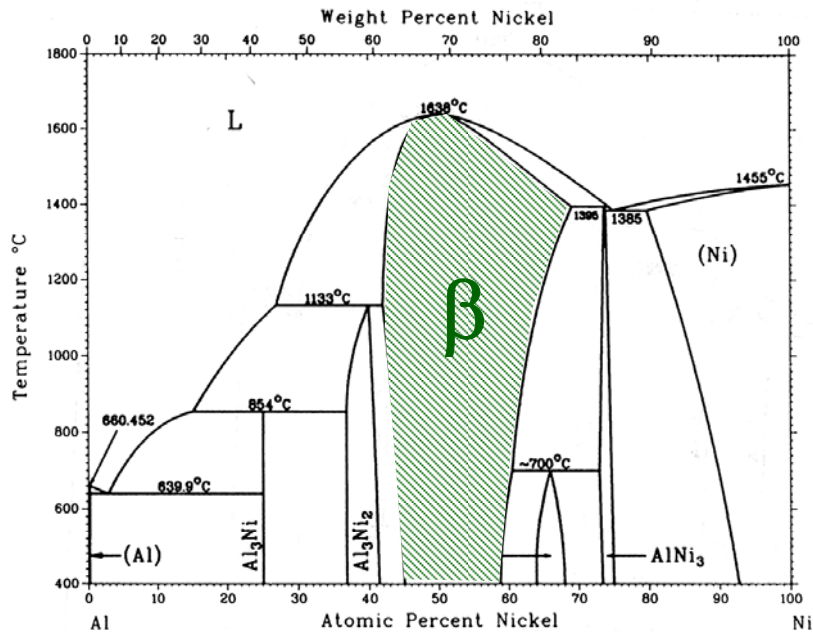
Al-Ni Phase Diagram



L1₂

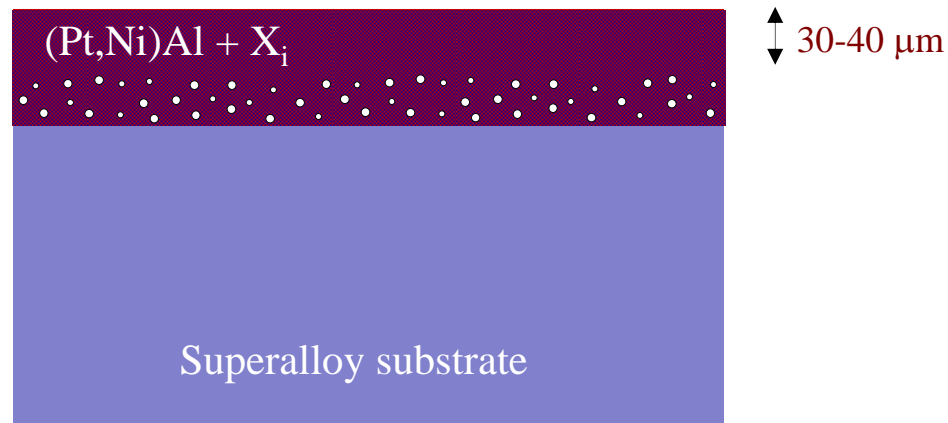
Ni-Al binary phase diagram:

Al-Ni Phase Diagram



B2

Commercial Pt aluminide coatings

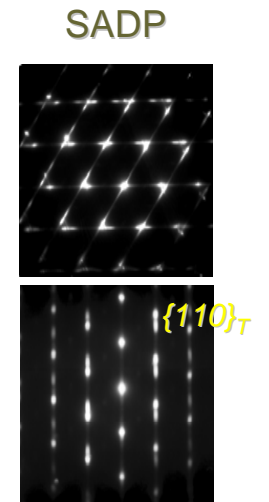
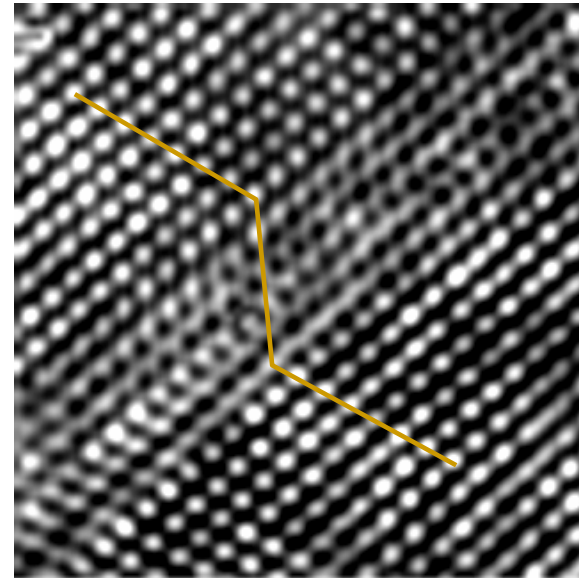
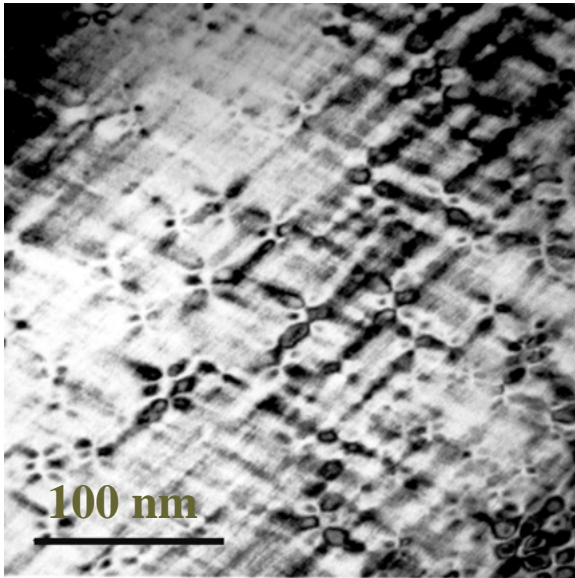
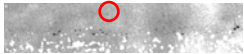


- Bond coat chemistry and microstructure effected by interdiffusion with substrate ... **reactive elements appear to be good!!**

TEM observations of diffusion aluminized coating

As-deposited

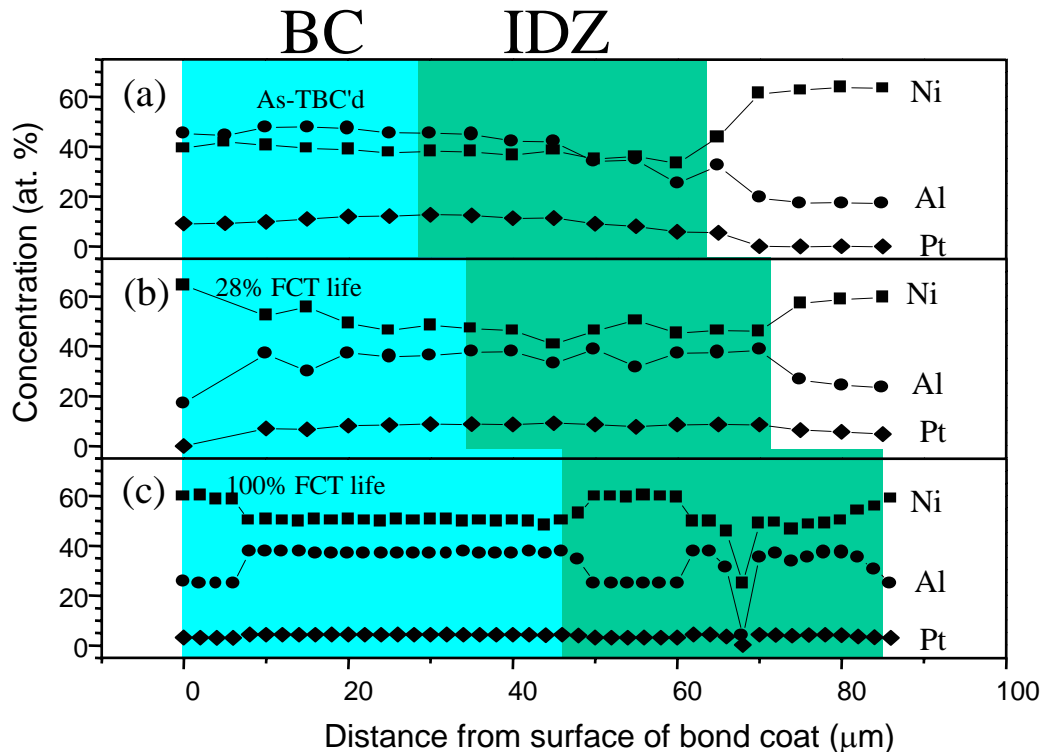
Thermal cycled



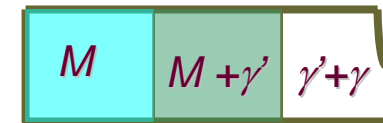
B2

L1₀ Martensite

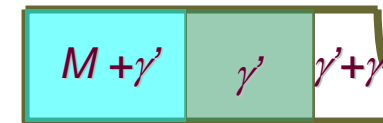
Compositional changes:



As-TBC'd



28% FCT life



100% FCT life

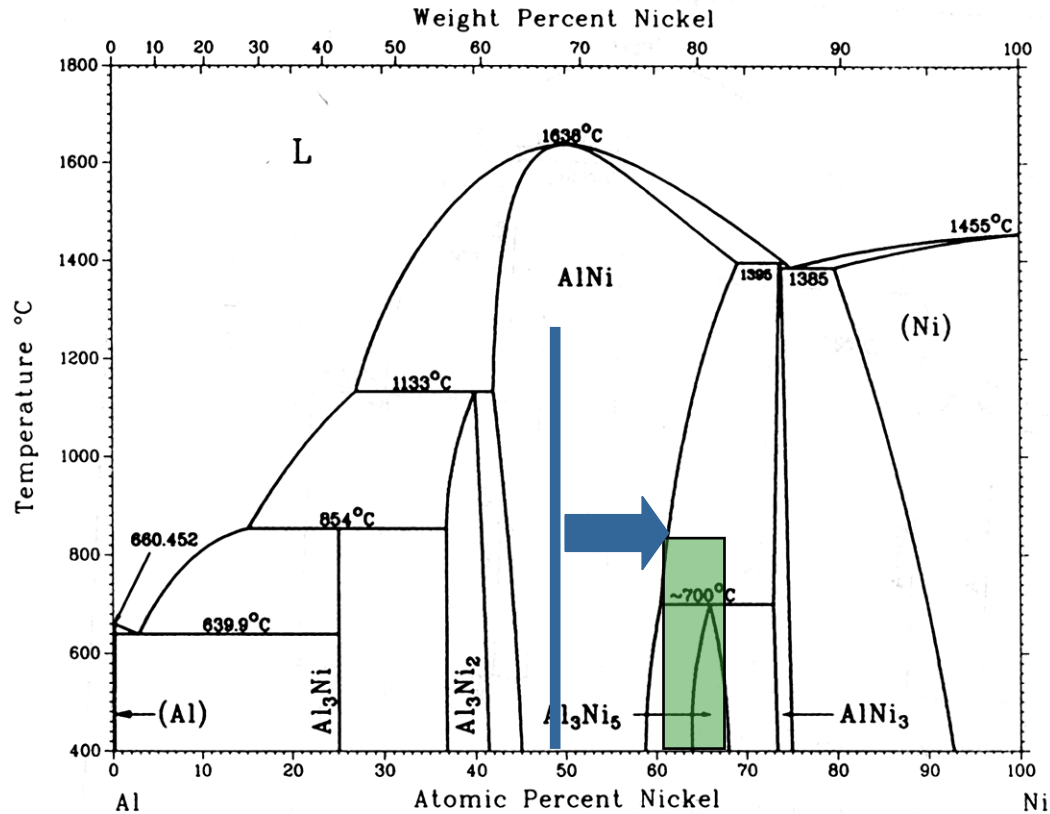
Sample	Ni	Al	Pt	Cr	Co	Ta	Re	W
0%	36.72	43.50	12.10	3.9	3.78	0	0	0
28%	46.01	35.92	8.09	4.45	5.11	0.28	0.049	0.057
100%	51.32	34.44	4.08	4.21	5.17	0.57	0.08	0.13

→ Ni diffuses outward

Bond coat evolution ...

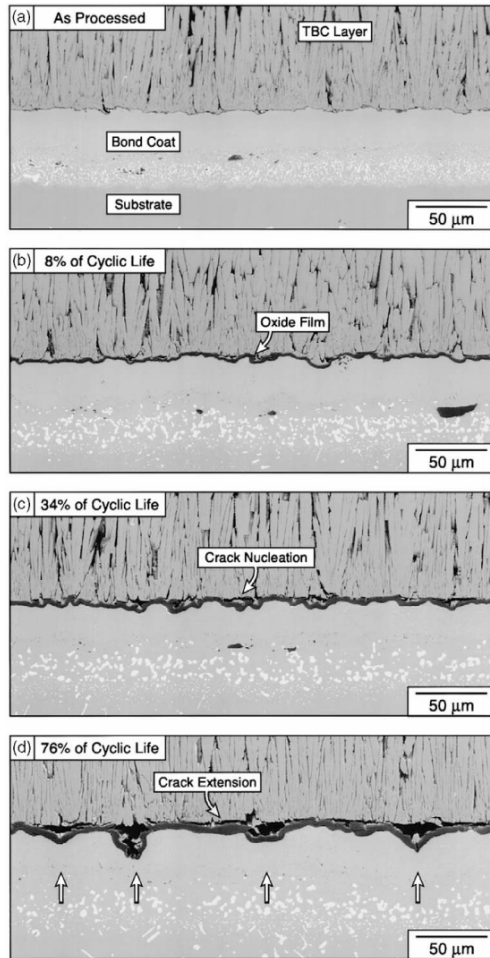


Al-Ni Phase Diagram



■ Martensite transformation has been reported in this composition range.
For example:
Smileck, *et al*, 1973, Metall. Trans.
Khadkikar, *et al*, 1993, Metall. Trans.

Failure by ratcheting and spallation



Key observations:

- Isothermal exposure is not the same as thermal cycling.
- TGO thickens, lengthens and roughens as a result of thermal cycling.
- Bond coat must creep to allow TGO to ratchet.
- Top coat cannot creep; it cracks instead

Advanced model of TGO ratcheting:

Balint-Hutchinson model

A special purpose multilayer code that takes input from micromechanical parameters and predicts the progressive development of undulations of the TGO layer upon thermal cycling.

- Key microstructural parameters:

$E_{\text{sub}}, \alpha_{\text{sub}}, E_{\text{bc}}, \alpha_{\text{bc}}, \gamma S_{\text{bc}}, (\text{creep rate})_{\text{bc}}, t_{\text{bc}}, \epsilon_{\text{mart}}, M_s, A_s,$
 $\alpha_{\text{tgo}}, E_{\text{tgo}}, (\text{growth rate})_{\text{tgo}}, (\text{creep rate})_{\text{tgo}}, \gamma S_{\text{tgo}}, t_{\text{tgo}},$
 $(\text{shape})_{\text{tgo}}, E_{\text{tbc}}, \alpha_{\text{tbc}}, (\text{creep rate})_{\text{tbc}}, \gamma S_{\text{tbc}}, \dots$

- *Note: property measurements and microstructural observations of bond coat are crucial to model development.*

*Measuring the mechanical properties
of diffusion aluminide bond coats*

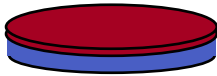
Bond coat microsample preparation:

Bond coat

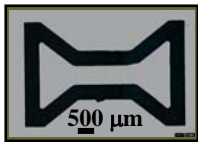
Substrate



600 μm slice is scalped from 1 inch diameter button using a wire EDM.



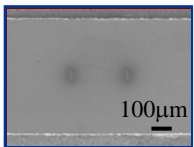
A lapping machine is employed to grind the superalloy side of the slice to get a uniform thickness of $\sim 150\mu\text{m}$.



A sinking EDM is then used to punch microsamples from each slice.



Faces of the microsample are polished to a mirror finish and a final thickness of 30~50 μm with TEM 'dimpler'.



Pt lines are deposited on both sides of the microsample using a Focused Ion Beam (FIB).

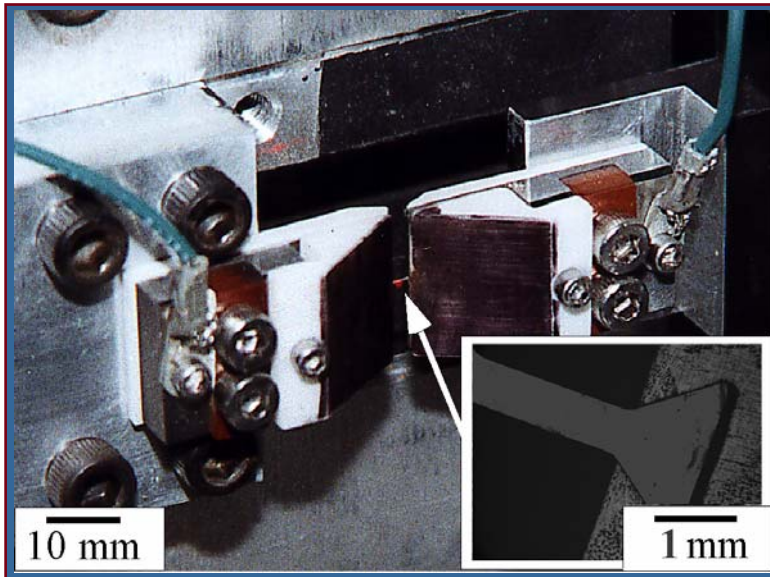
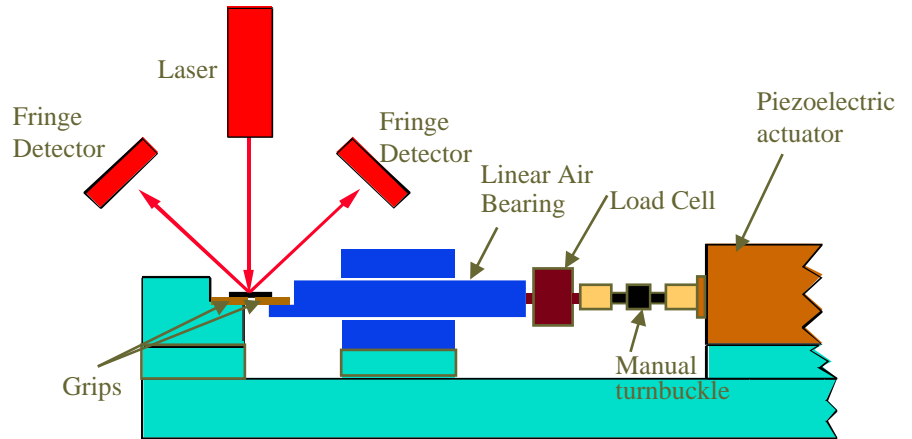
Microsample testing

- Microsamples:



3.5 mm x 1.2 mm x 25 μm
(overall)

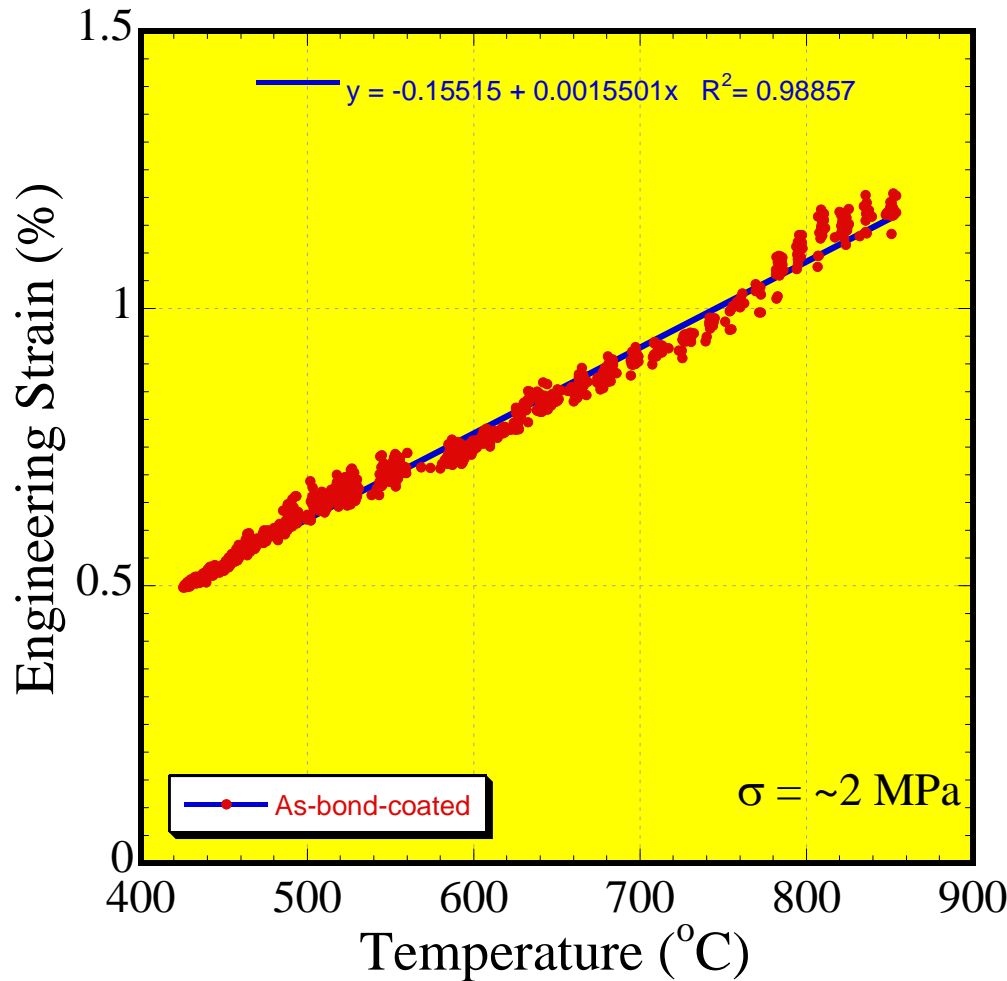
250 μm x 500 μm x 25 μm
(in gage)



- Temperature range of 25-1200°C can be achieved by resistive heating.

- ISDG provides a strain resolution of better than 5 μstrain .

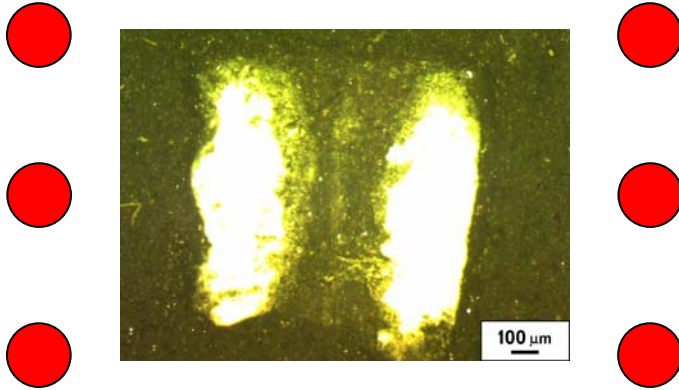
Measuring bond coat CTE (T):



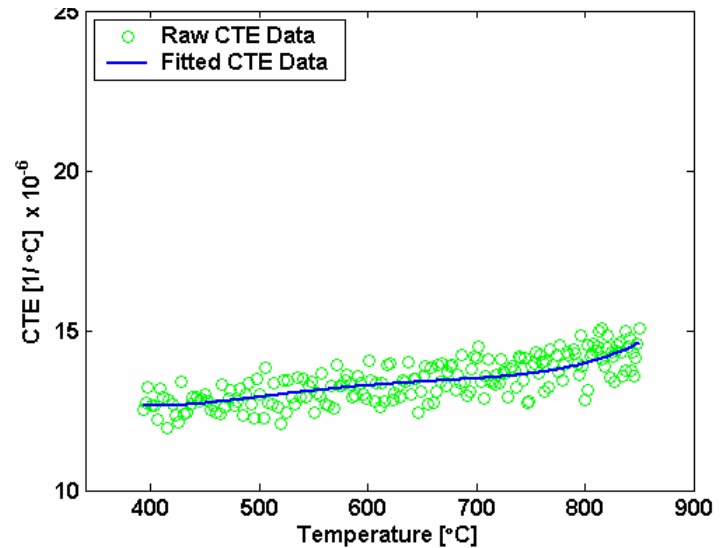
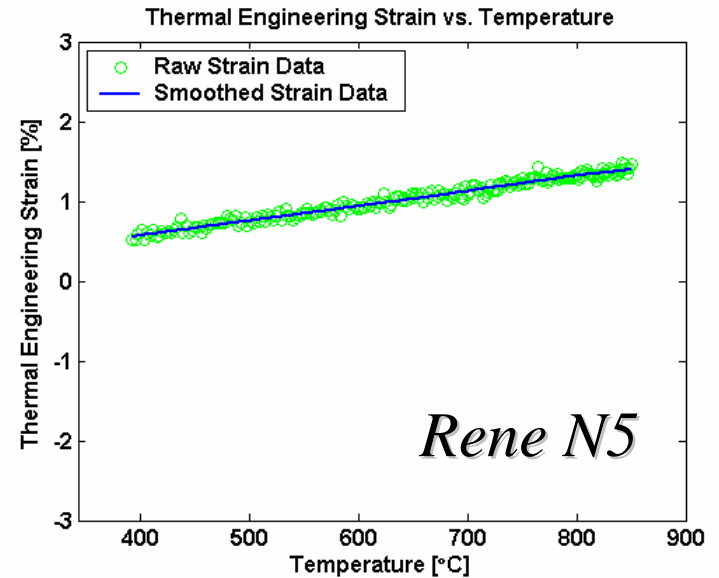
- CTE of as-coated bond coat has been determined to be **15.5 ppm °C⁻¹** between 400°C and 850°C.

- CTE measurement above 850°C was hindered by creep.

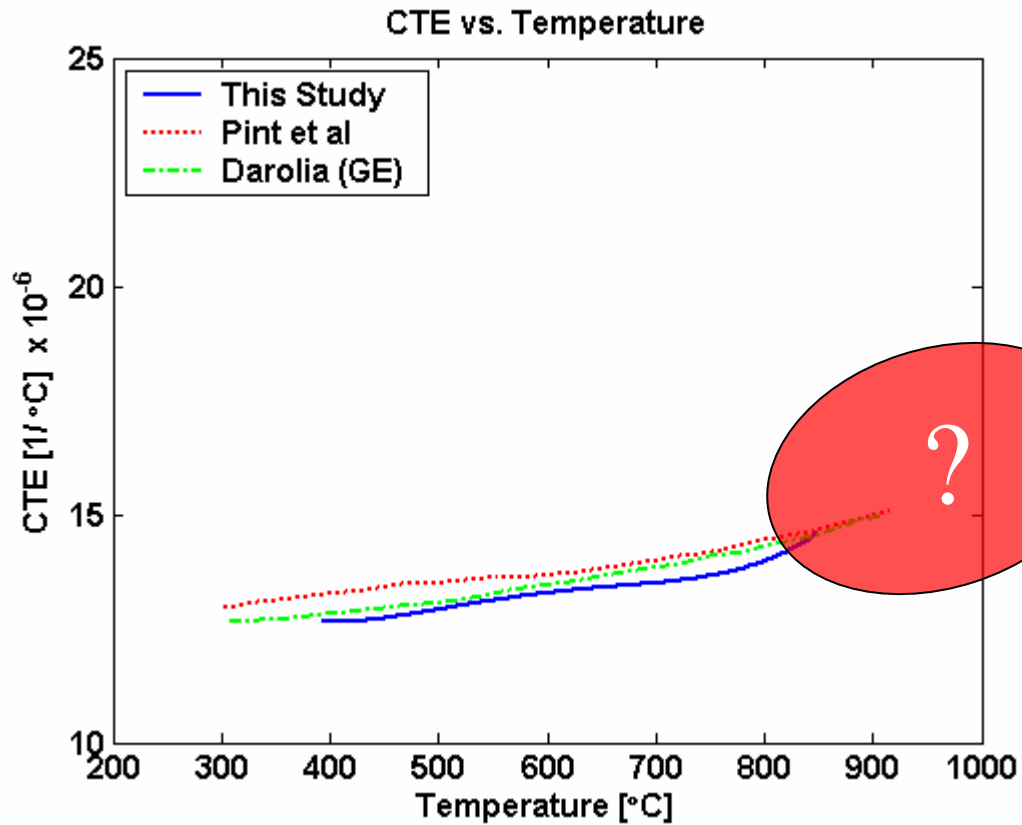
Optical CTE measurements



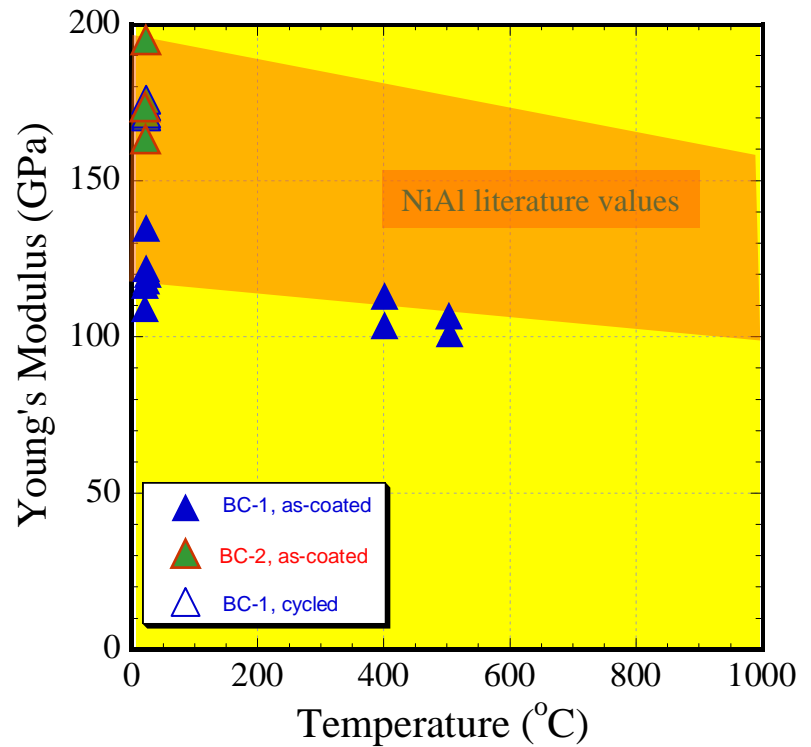
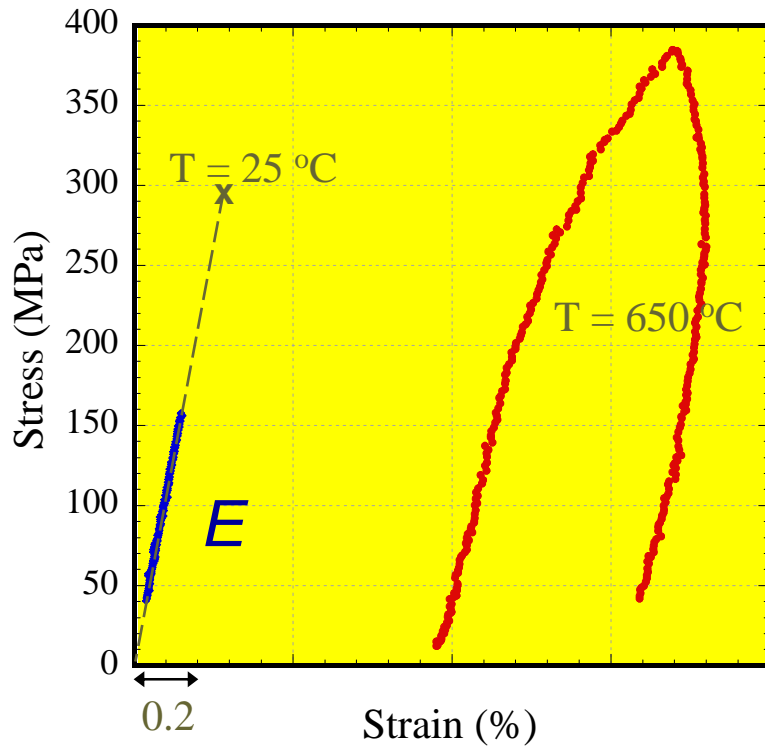
$$CTE = \frac{d\varepsilon_{xx}(T)}{dT} = \frac{d}{dT} \left(\frac{\partial u}{\partial x} \right)$$



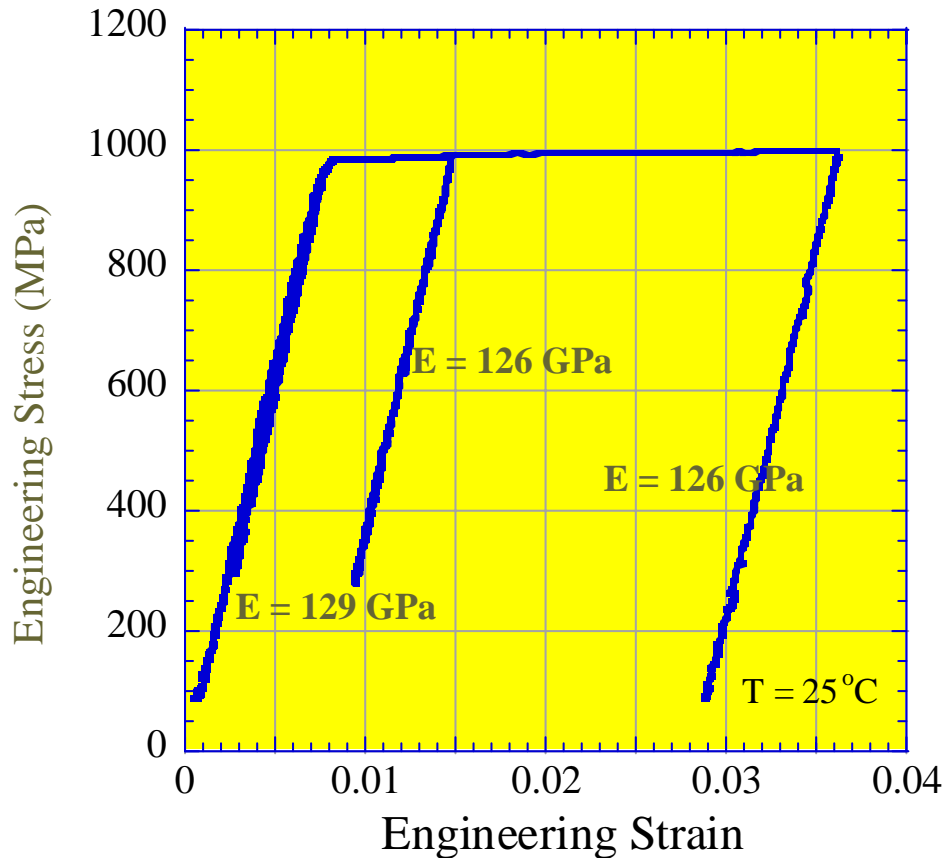
Optical CTE measurements



Measuring bond coat $E(T)$:



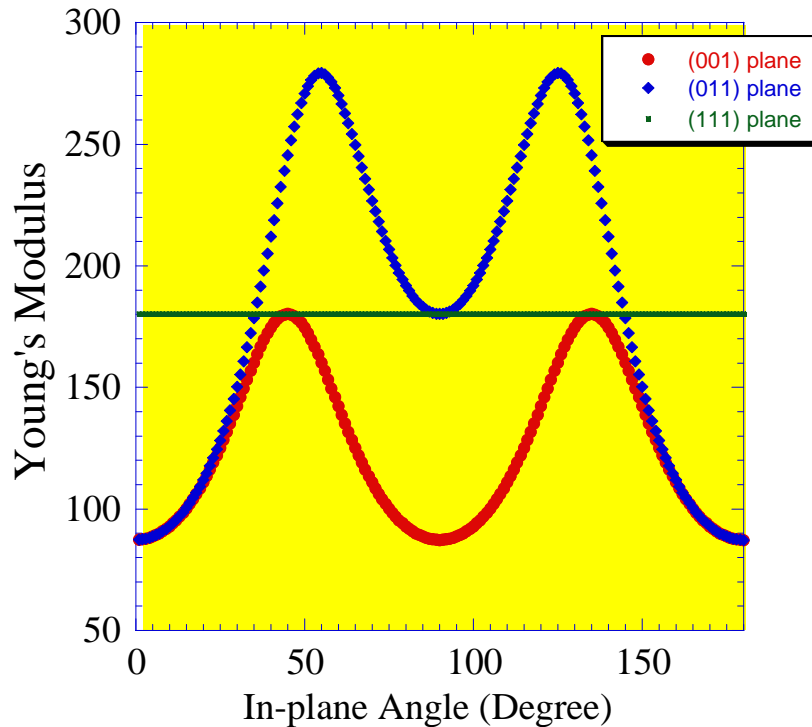
Microsample tests of Rene N5 :



- Modulus of [100] oriented single-crystalline Rene N5 microsamples measured to be 126 ± 3 GPa (8 measurements).
- GE reported modulus to be $E = 129$ GPa.

Texture effects on E:

The Elastic Constants of NiAl (Ref. Rusovic <i>et al</i> , 1977)		
C_{11}	C_{12}	C_{44}
199 GPa	137 GPa	116 GPa

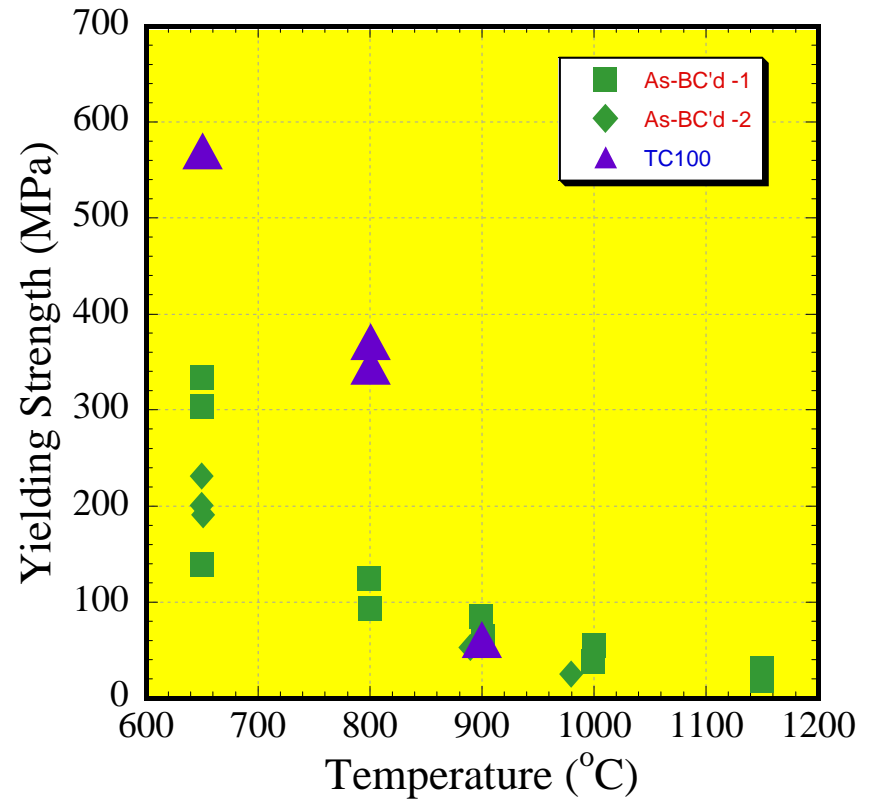
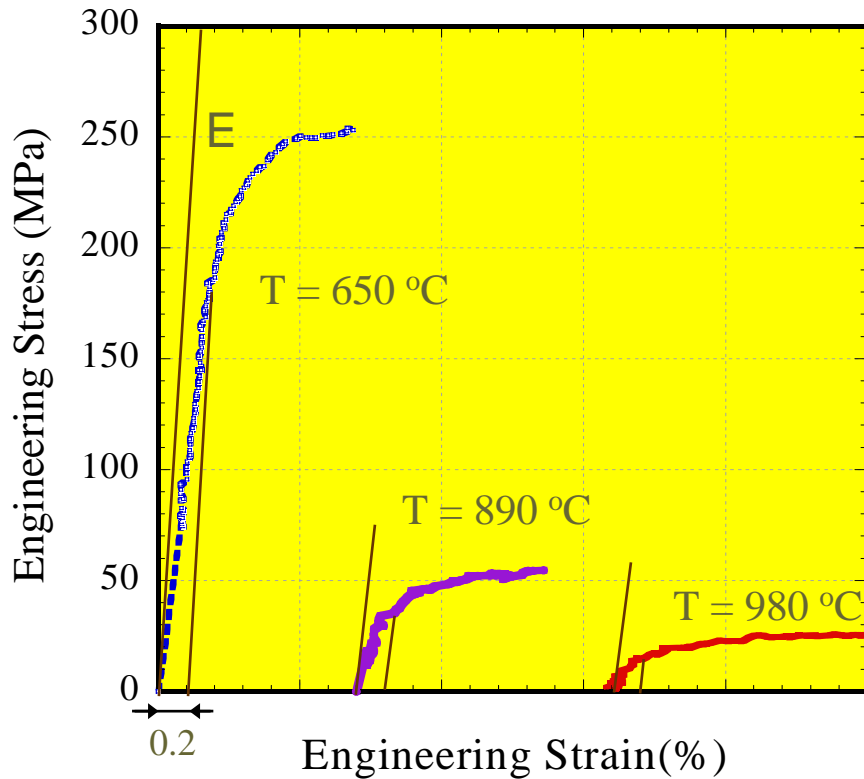


The Average E in Certain Texture of NiAl

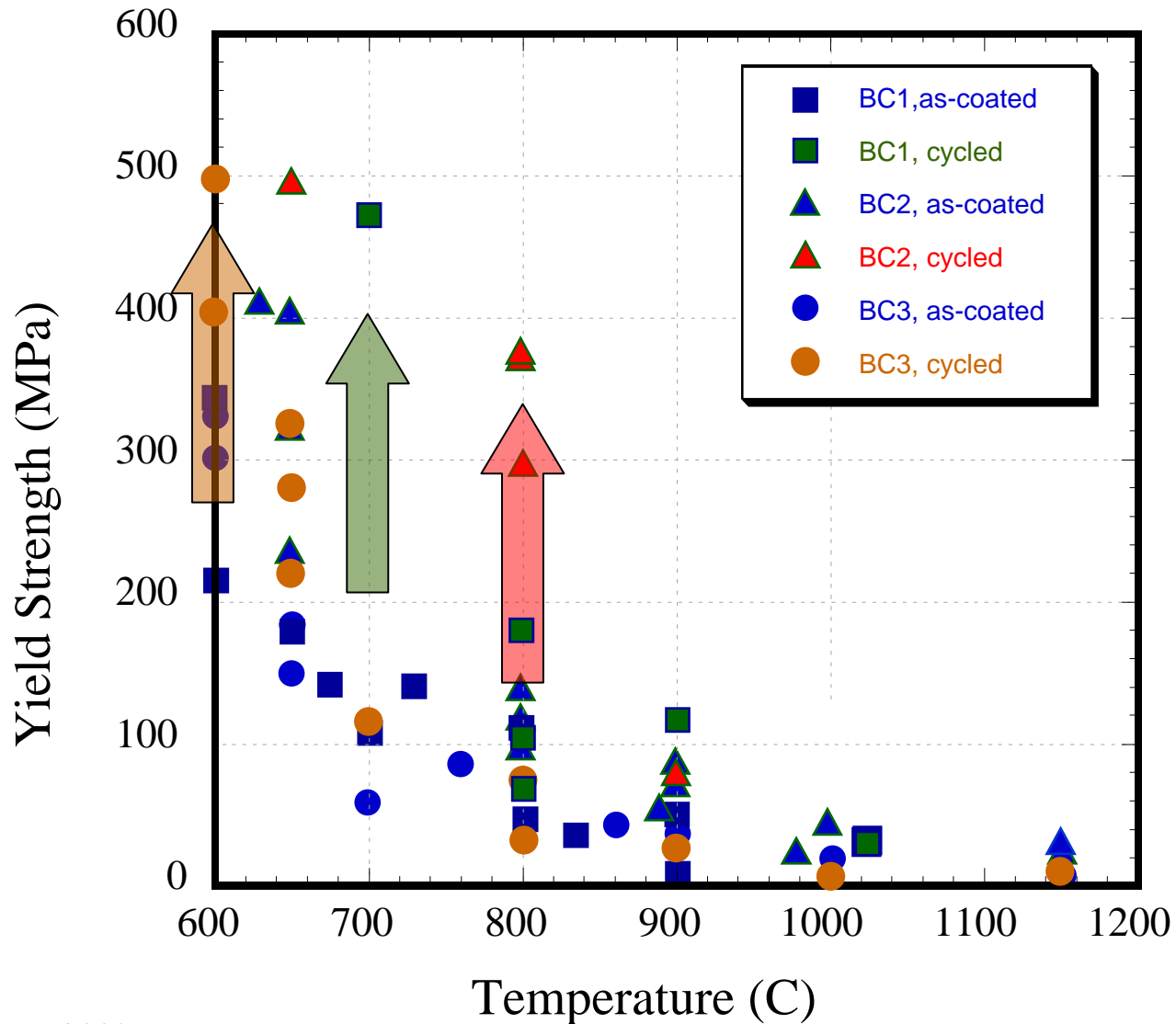
E(GPa)	(001) plane	(011) plane	(111) plane
Voigt	125	184	181
Reuss	117	159	181

- Each angle corresponds to one certain orientation in that plane.
- The measured value of E is comparable to that of NiAl with a [001] texture.
- X-ray texture determination did not evidence any obvious out-of-plane texture of bond coats.

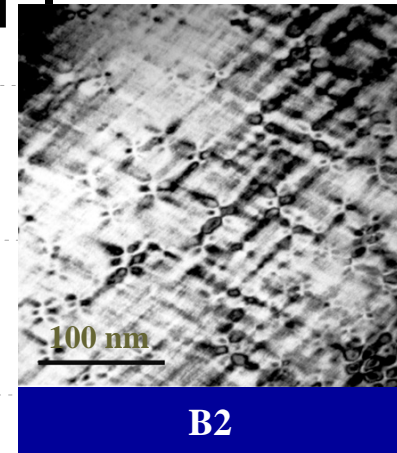
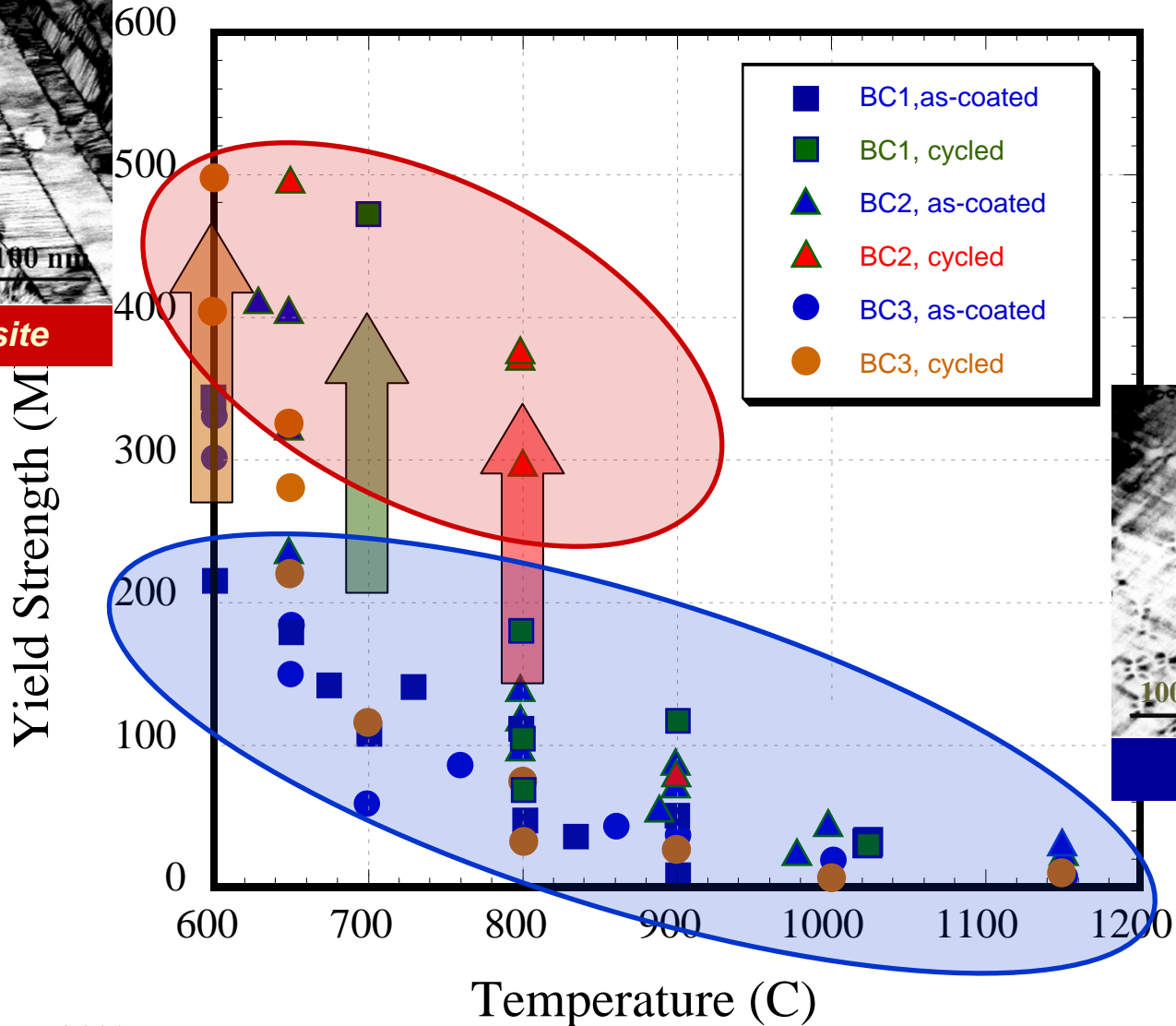
Measuring bond coat $\sigma_{\text{yield}}(T)$:



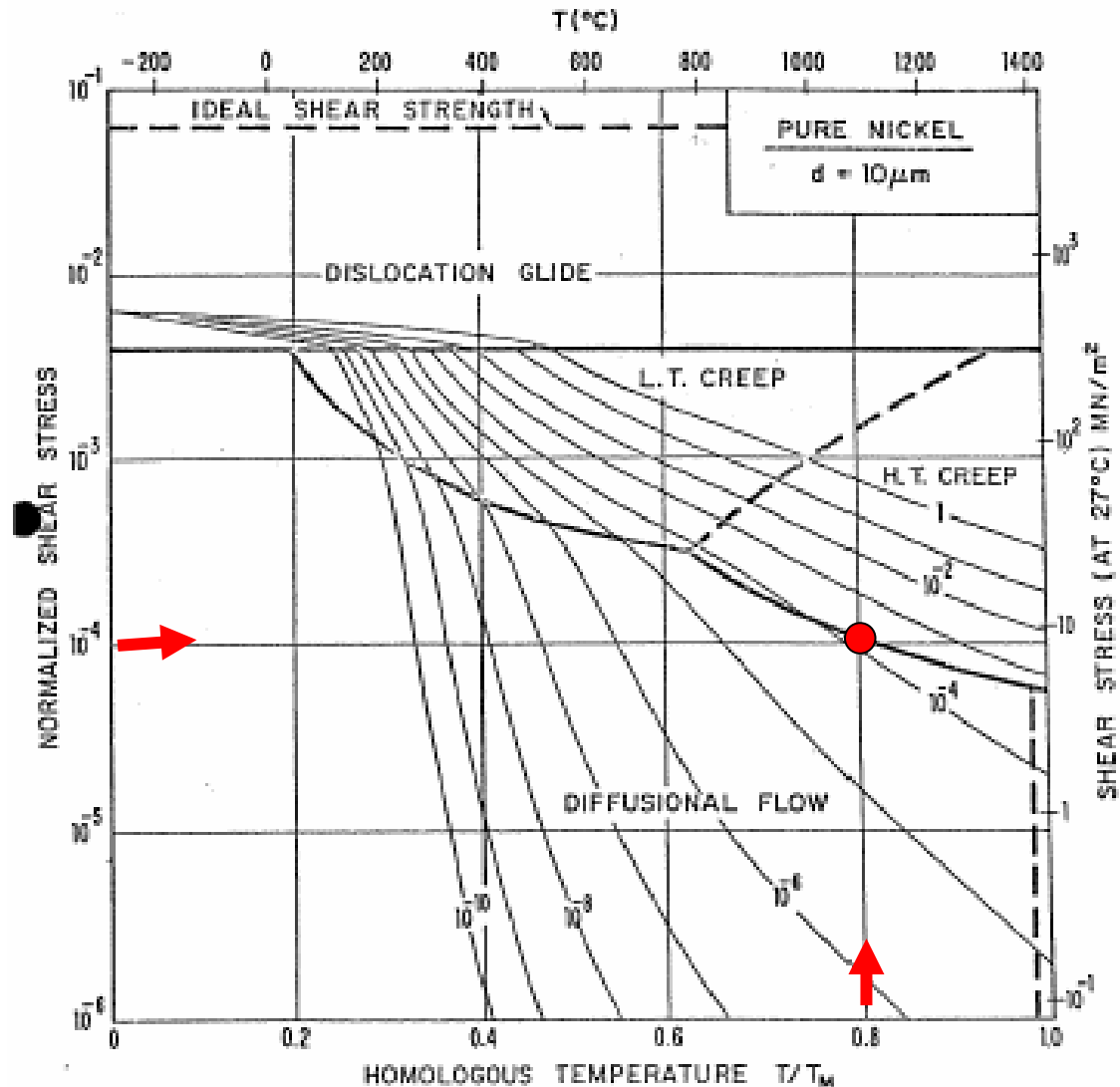
Effect of thermal cycling



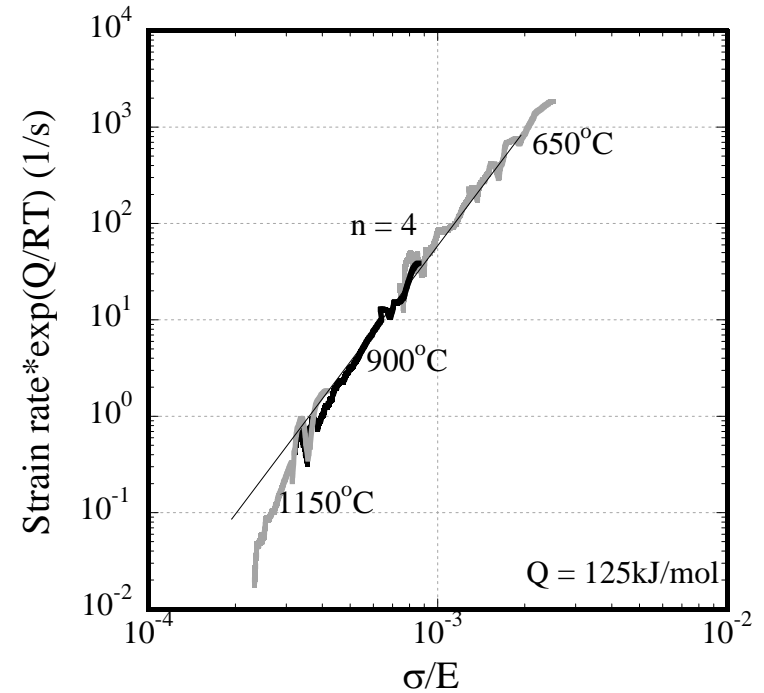
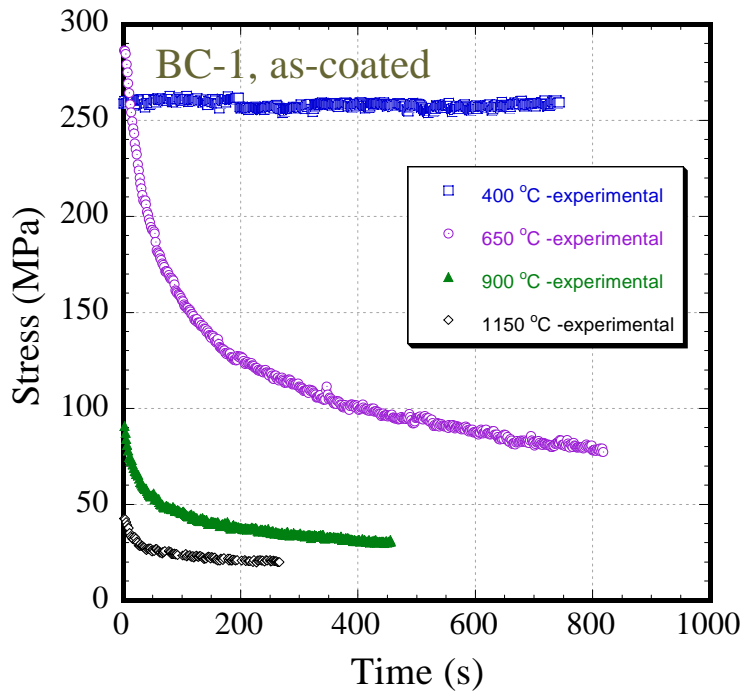
Effect of thermal cycling



High T deformation

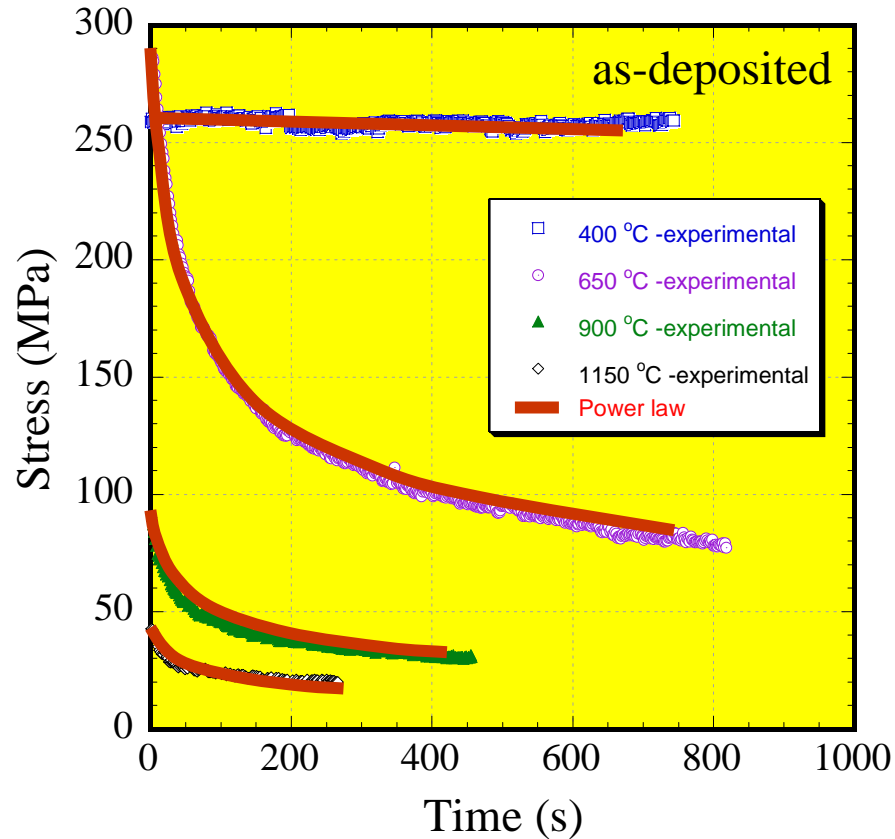


Stress relaxation behavior:



- Empirical fit suggests that Q_{creep} is only half of Q_D for NiAl and $n = 4$.

Stress relaxation behavior



Empirical fit:

$$\dot{\epsilon}_{pl} = -\dot{\sigma}/E_{\text{machine}} = 1.2 \times 10^{14} (\sigma/E_{\text{sample}})^4 \exp(-125(\text{kJ/mol})/RT)$$

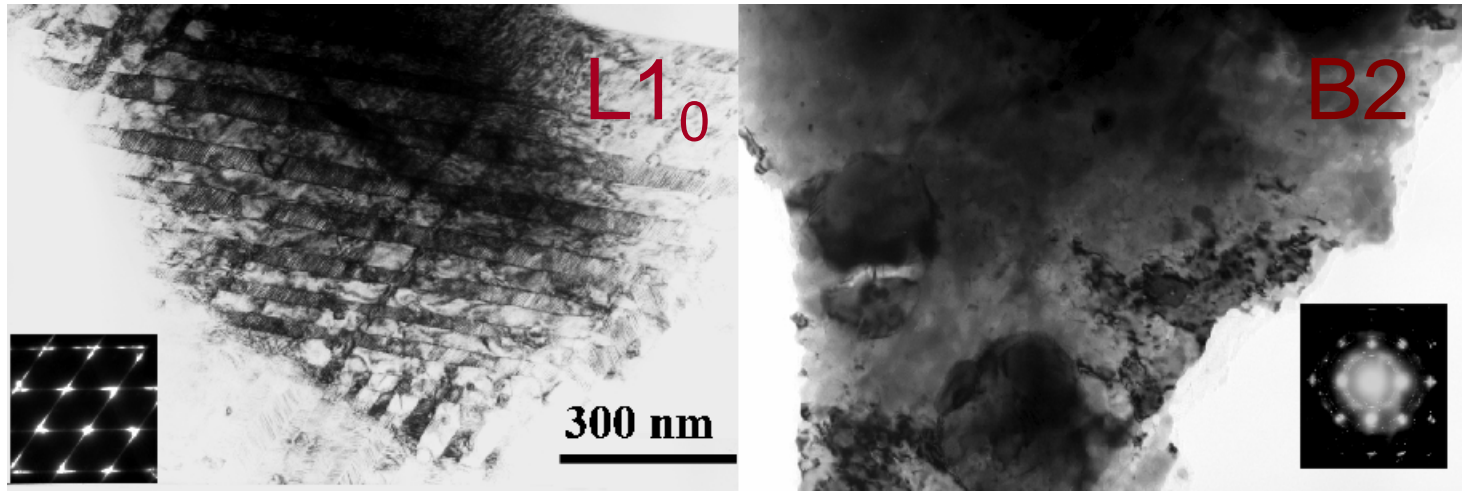
*Characterizing the
microstructural changes in
diffusion aluminide bond coats*

In-situ TEM observations:

25°C

->

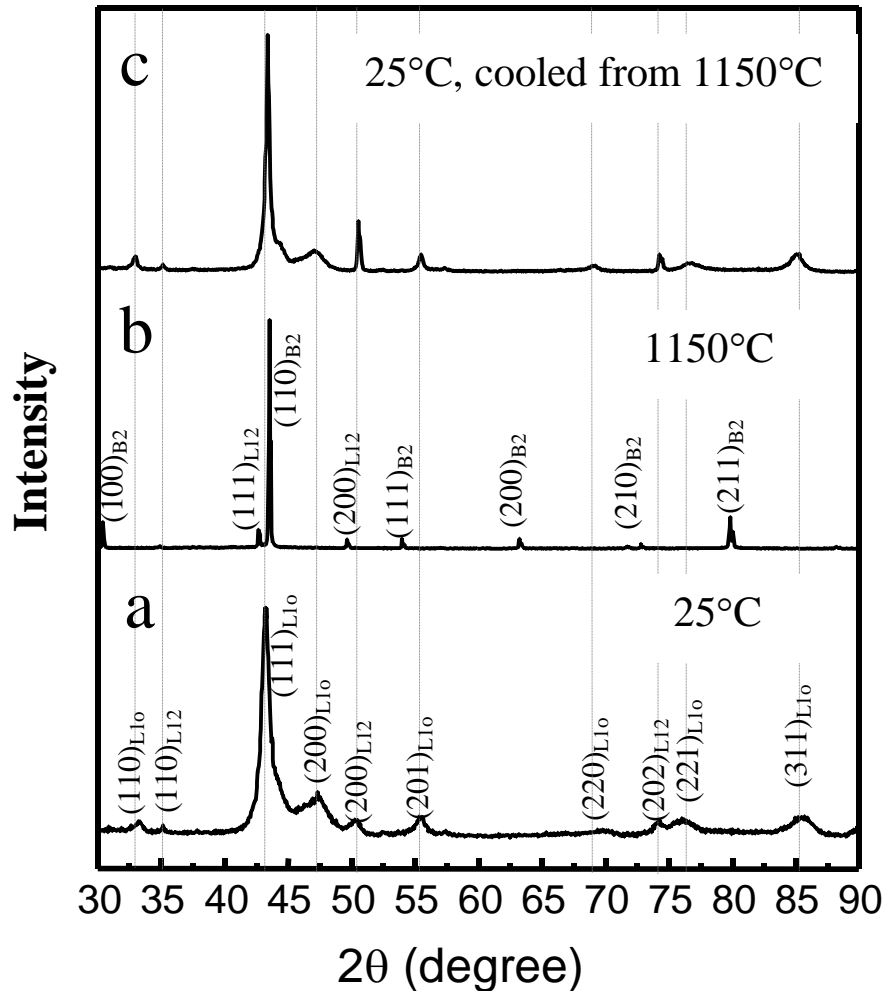
900°C



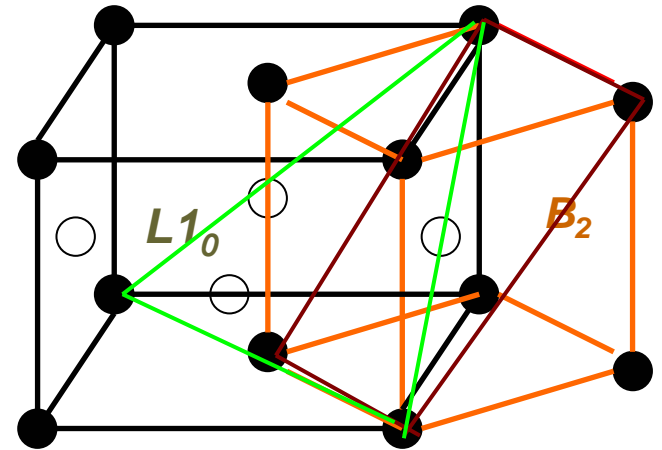
Transformation from martensitic $L1_0$ to $B2$ observed at approximately 800°C.

In situ heating X-ray diffraction:

Reversible transformation

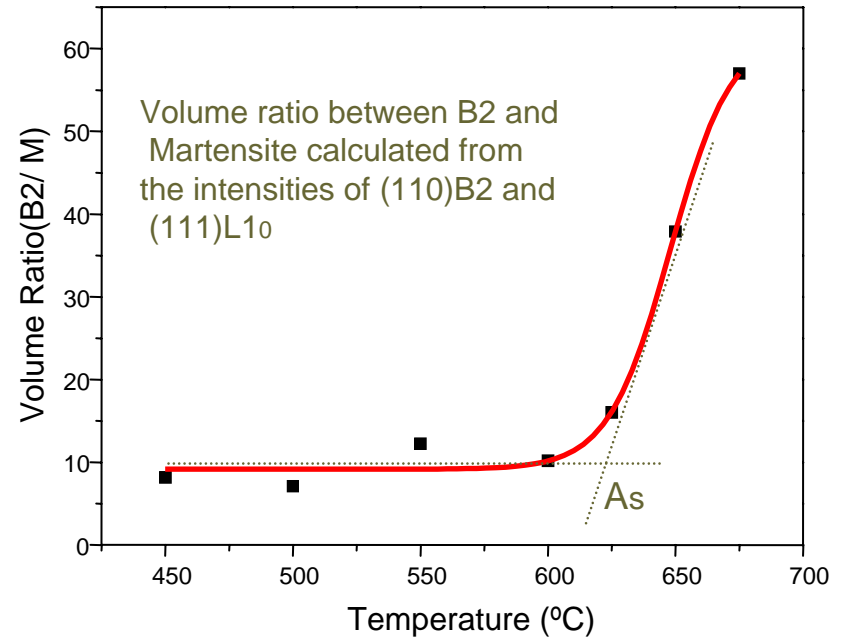
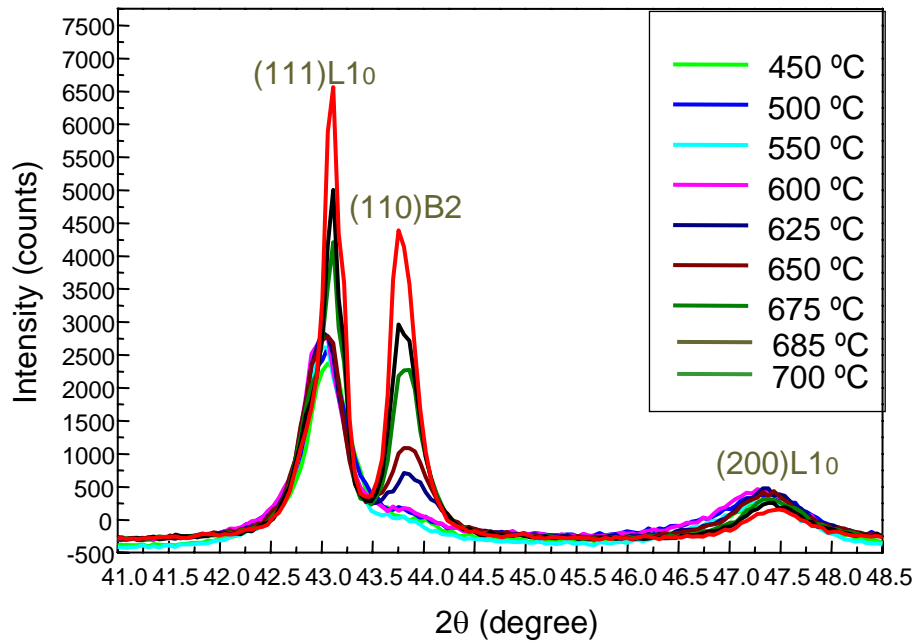


Crystallographic relationship between B_2 and $L1_0$



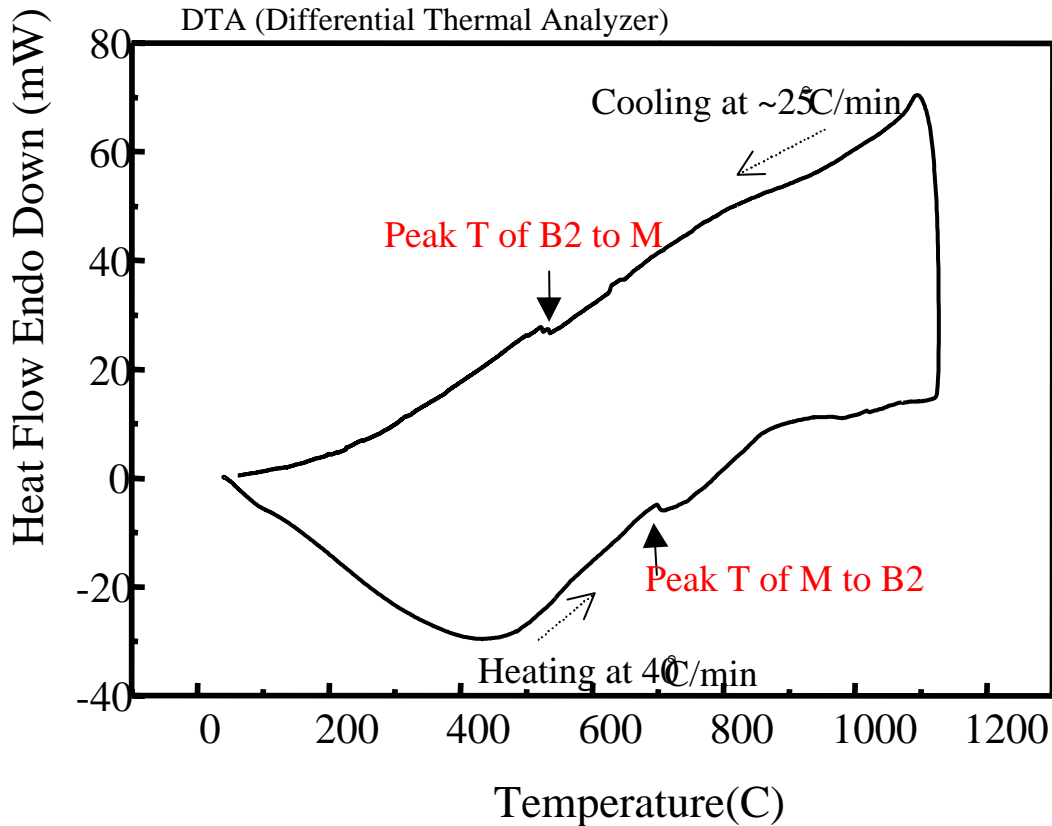
$$(011)_{B2} // (11-1)_{L1_0}$$

Transformation to B2:



The A_s temperature is approximately 620°C.

Martensite transformation temperatures:

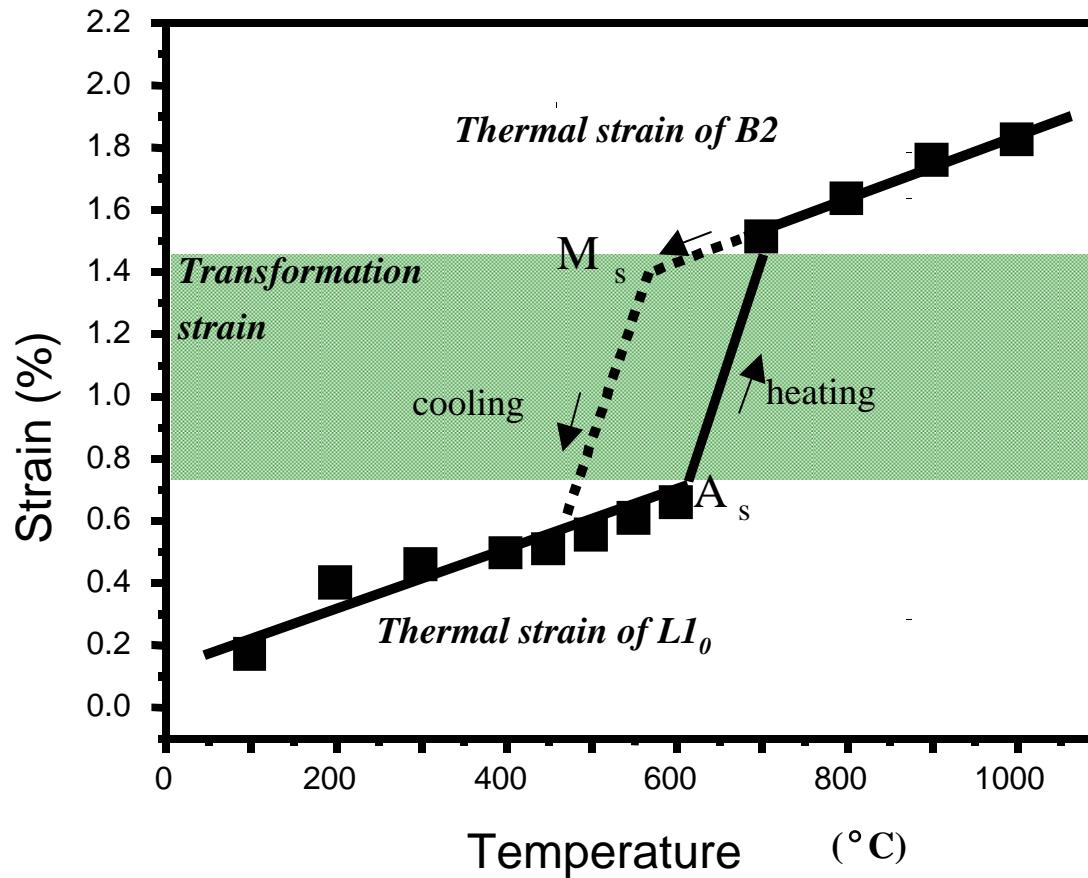


➤ The M to B2 transformation occurs at $600\text{-}700^{\circ}\text{C}$

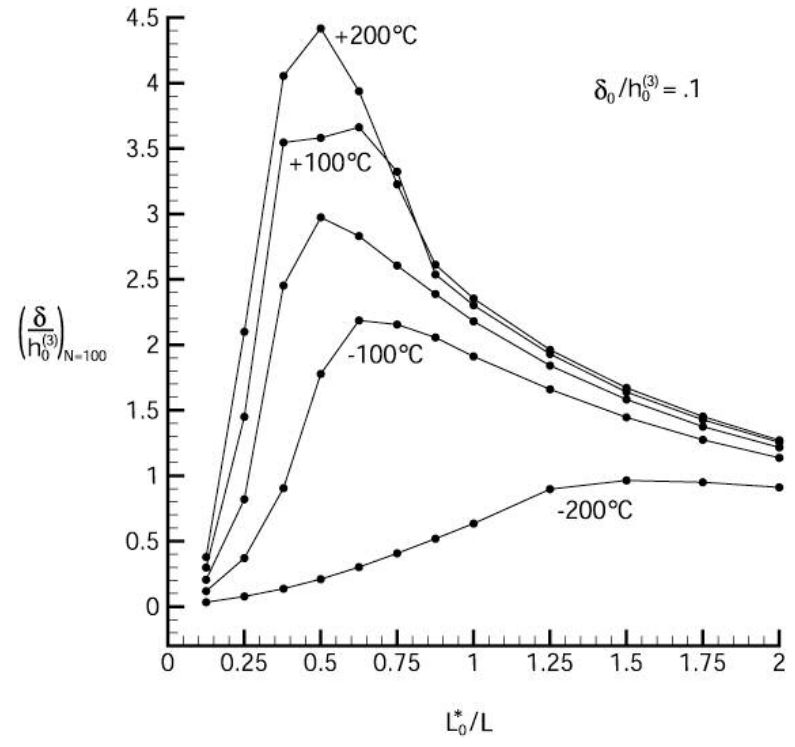
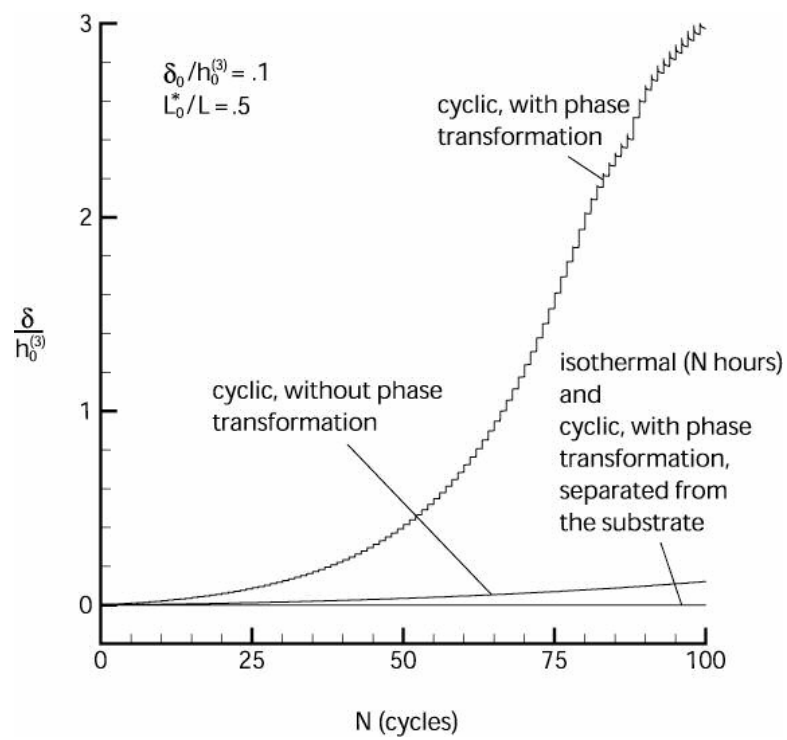
➤ The B2 to M transformation occurs at $550\text{-}650^{\circ}\text{C}$

➤ M_s is approximately $40\text{-}50^{\circ}\text{C}$ less than A_s

Thermal and transformation strains:



Effect of martensitic transformation



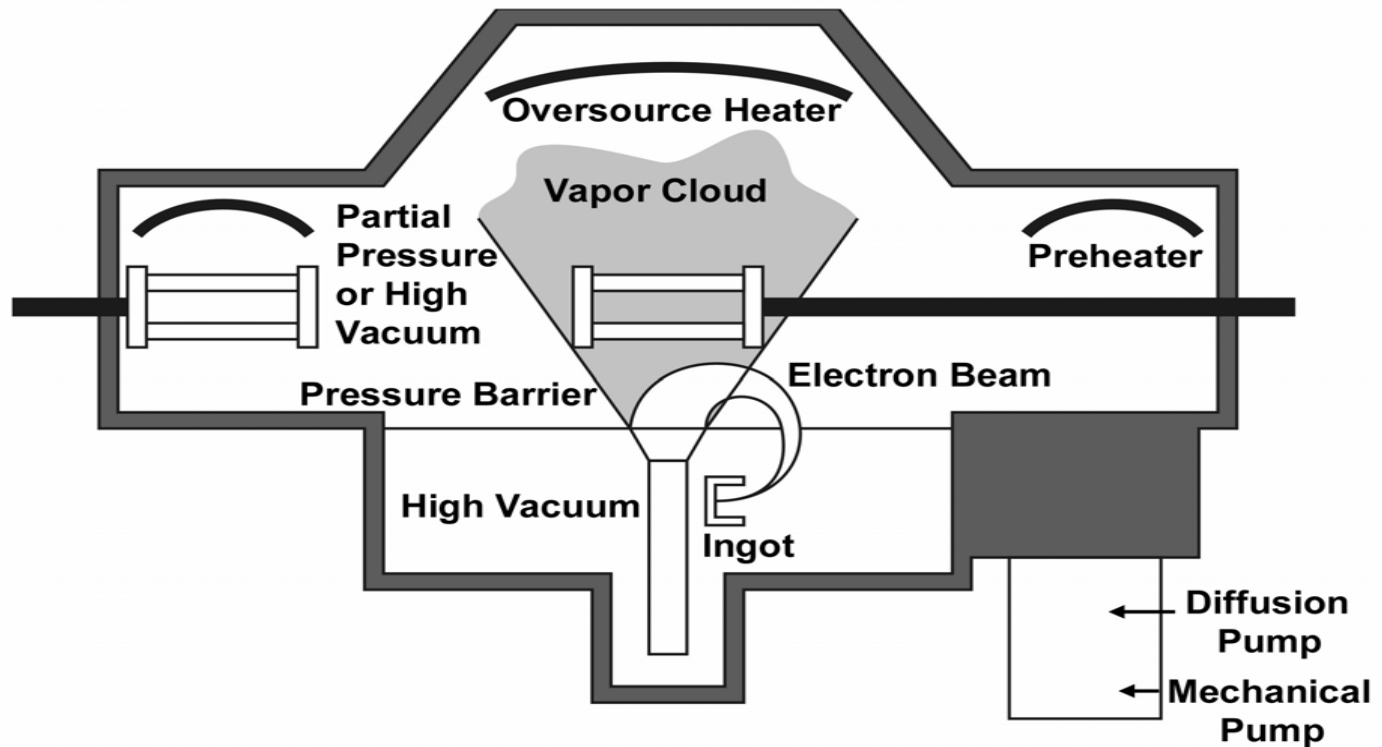
Strategies for bond coat design

- Improve oxidation resistance and slow TGO formation.
- Increase bond coat strength.
- Alloy to avoid martensitic and other phase transformations.

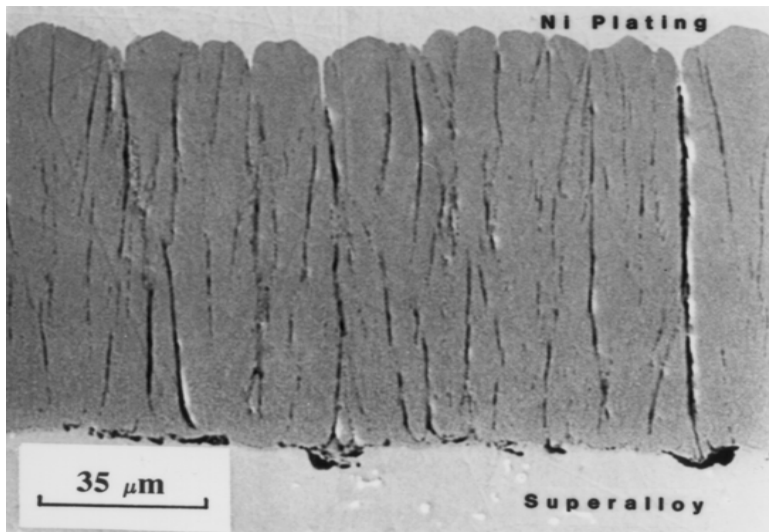
Overlay coatings for superalloys

- Developed to allow for greater flexibility in bond coat compositions.
 - Addition of reactive elements known to be beneficial
 - Peg formation, S gettering, increased TGO adhesion ???
 - Can tailor the phases present in the bond coat
 - $\beta + \gamma$, $\beta + \gamma'$, $\gamma + \gamma'$, etc.
- Requires deposition
 - Initially PVD
 - More commonly now LPPS

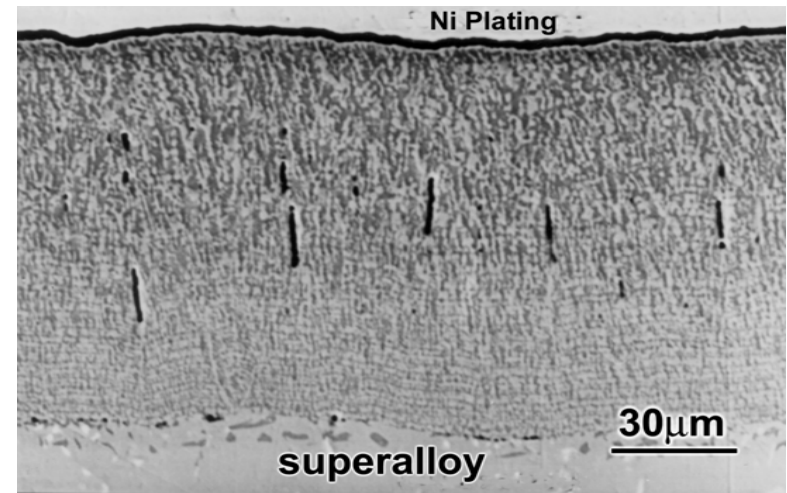
Schematic of an EBPVD process



EBPVD coatings

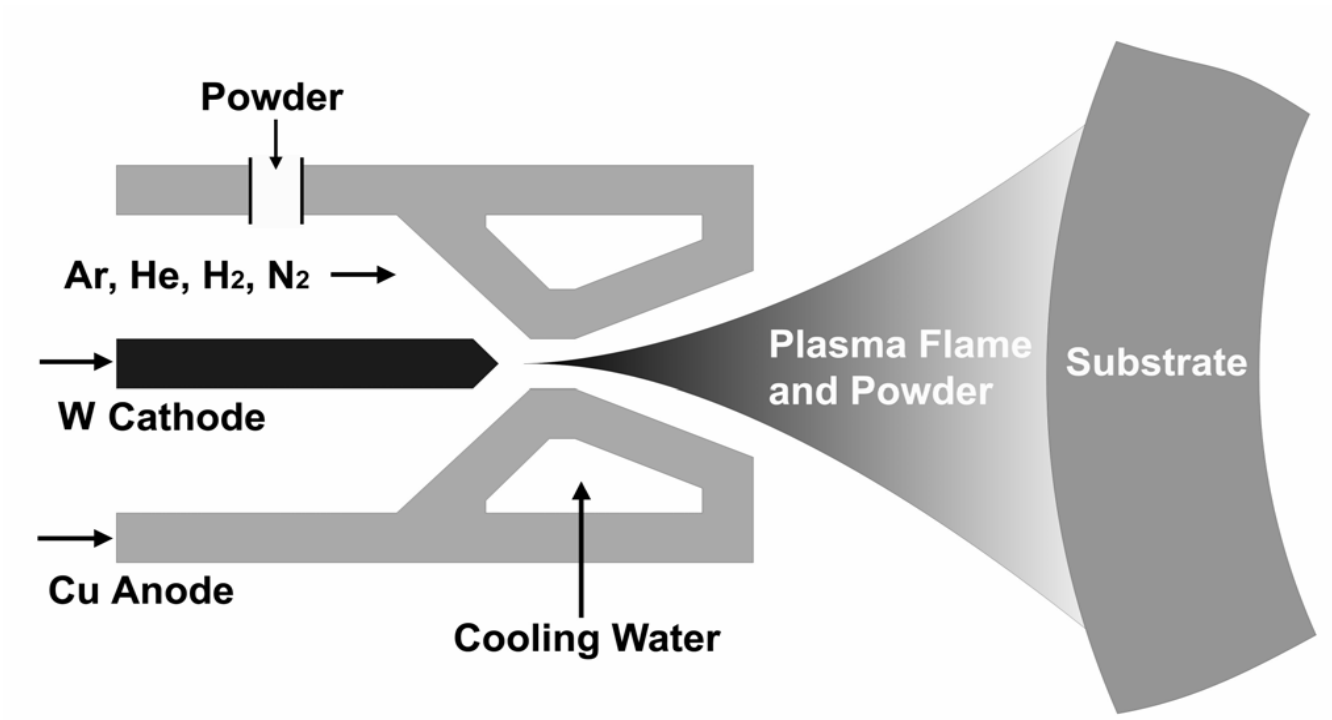


CoCrAlY coating as-deposited

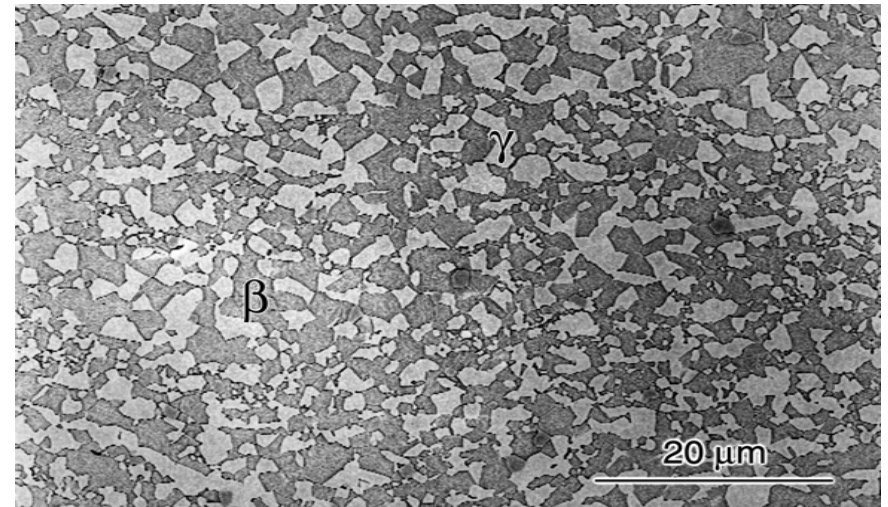
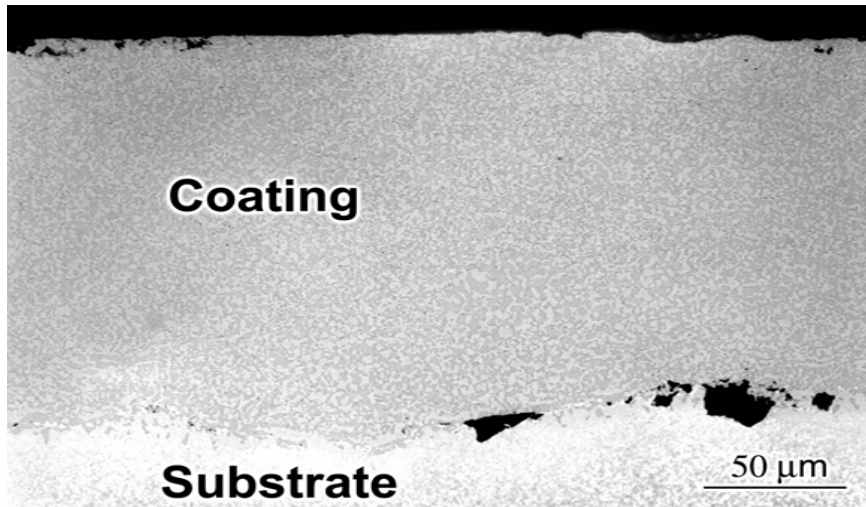


CoCrAlY coating after peening and heat treatment

Schematic of a plasma deposition system



NiCoCrAlY argon-shrouded plasma sprayed coating



NiCoCrAlY coating after peening and heat treatment

Aero history of overlay coatings

• FeCrAlY

- Alloy merged from GE nuclear programs (1964)
- P&W applied (EBPVD) as a coating (1970)
- Limited at high T by formation of a brittle NiAl layer

• CoCrAlY (1972)

- Useful oxidation resistance but too brittle

• NiCrAlY (1973)

- Limited hot corrosion resistance but ductile

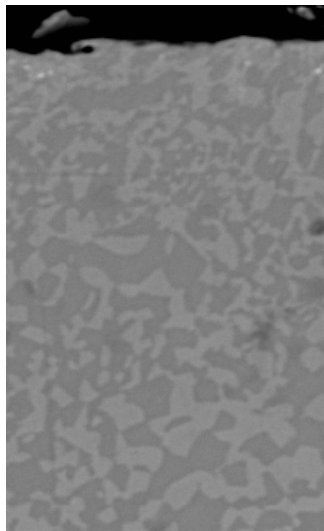
• NiCoCrAlY (1975; 1986)

- Good compromise; 40+ patented MCrAlY's

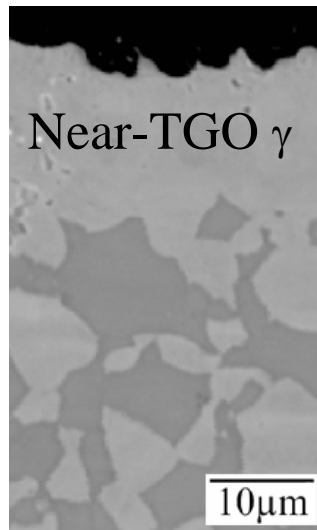
Microstructural observations of
Pratt & Whitney's "two-phase"
NiCoCrAlY(Hf,Si) bond coat

Effect of thermal cycling

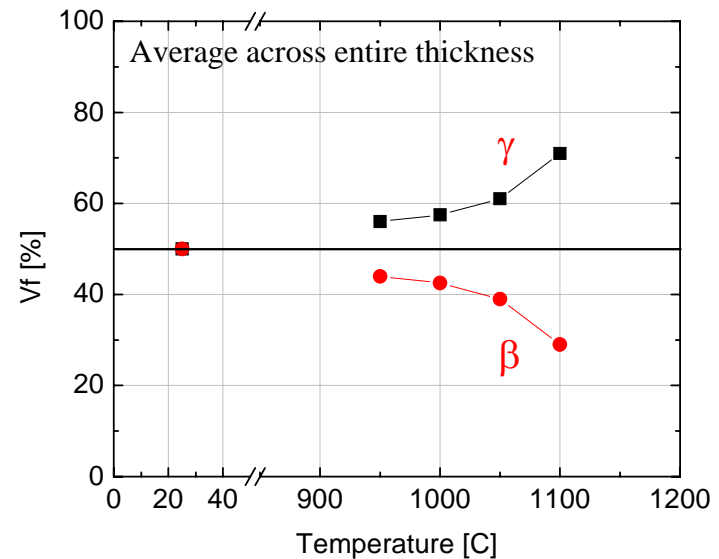
As-received



100 hrs @ 1100°C

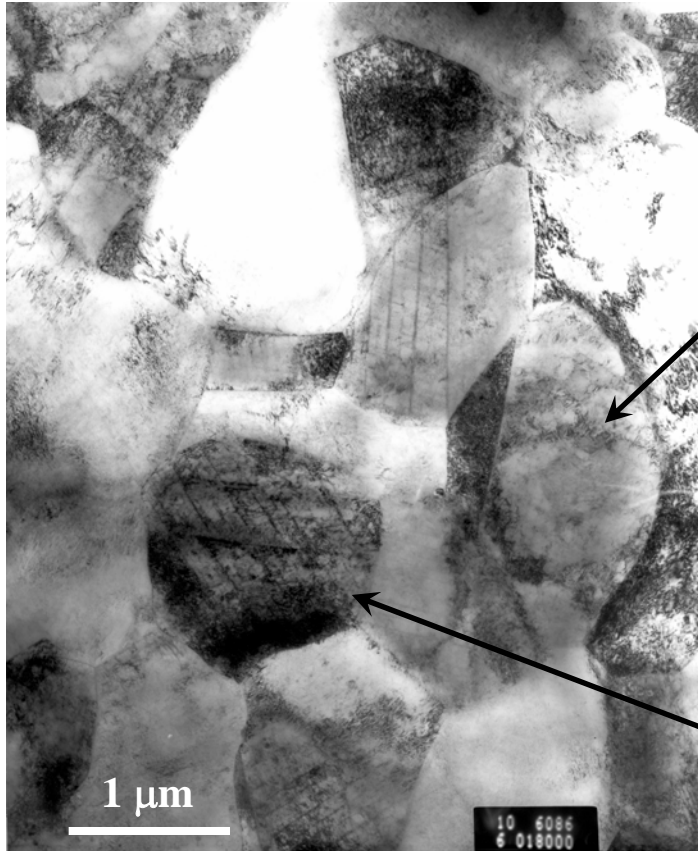


100 hrs @ T_i

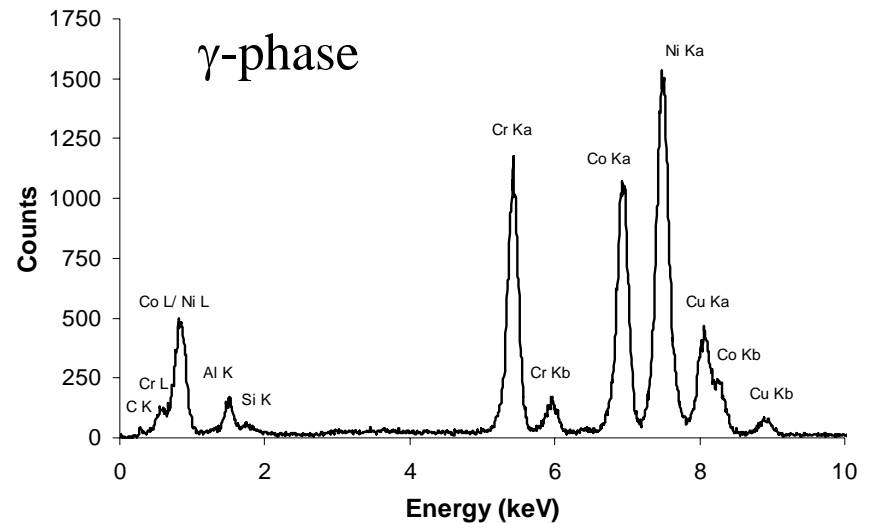
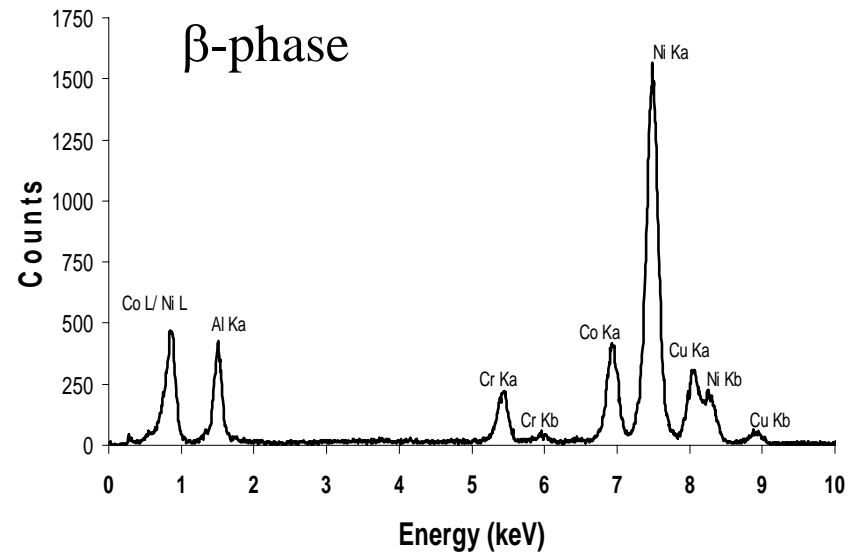


“two-phase bond coat”
(β -NiAl + γ -Ni)

TEM observations of the bond coat

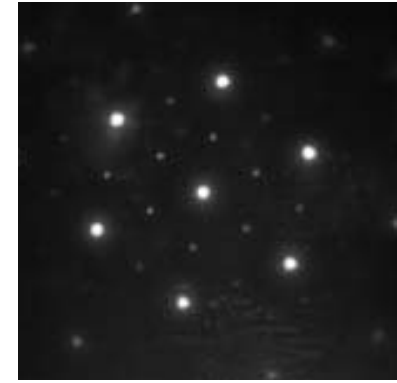
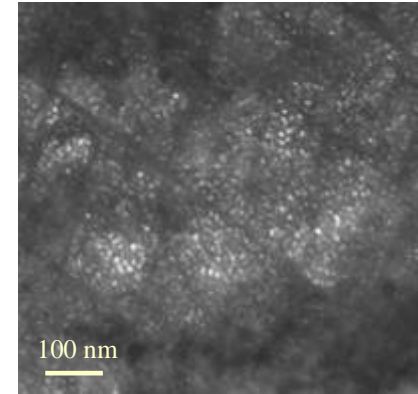
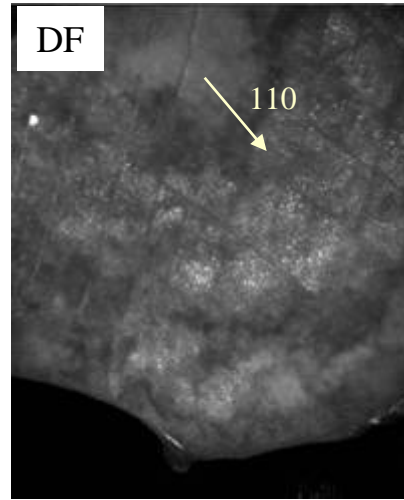
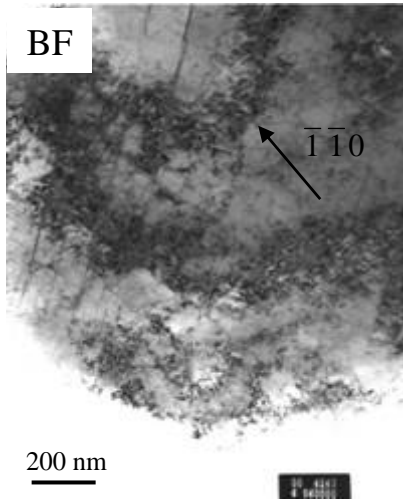


As-received NiCoCrAlY

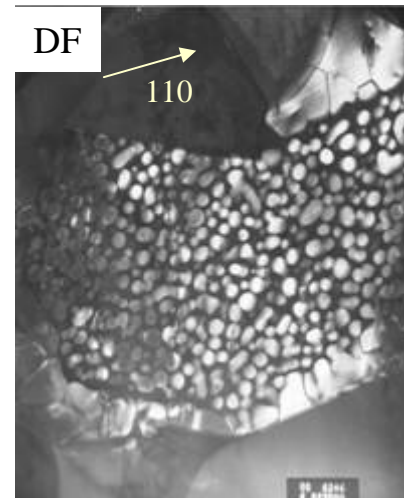
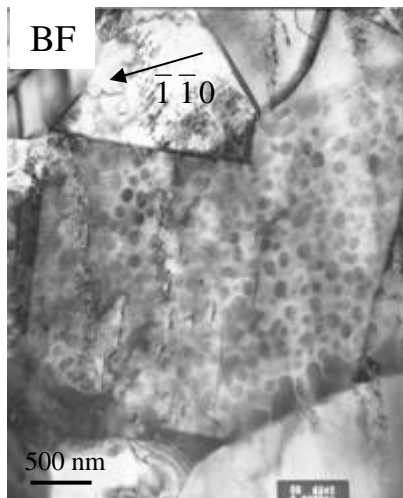


TEM observations of the γ grains:

As-received

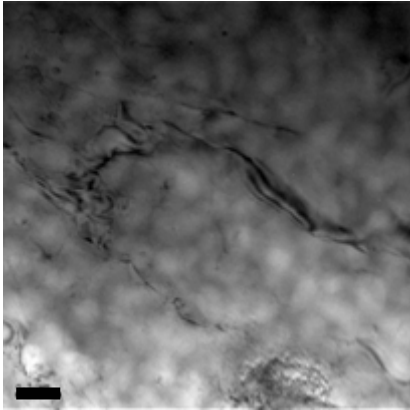


ELTB



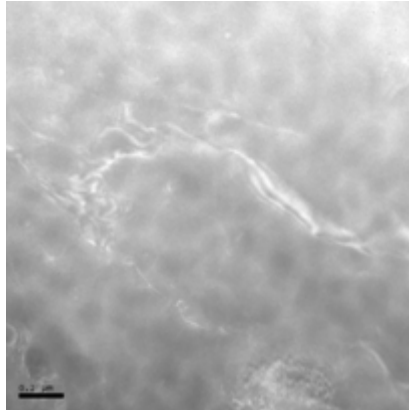
- γ grains filled with very fine γ' precipitates
- modest coarsening suggests the γ' dissolves at T.

EFTEM of γ' in the γ grains:

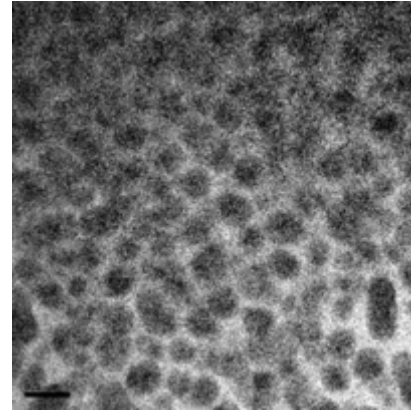


200nm

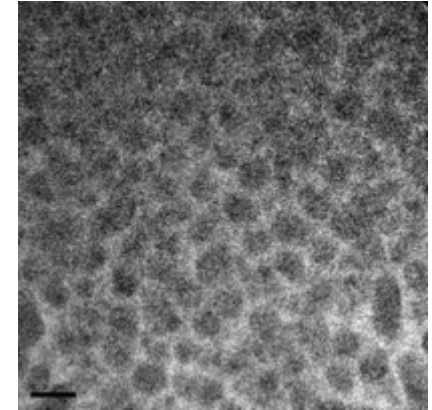
Elastic image



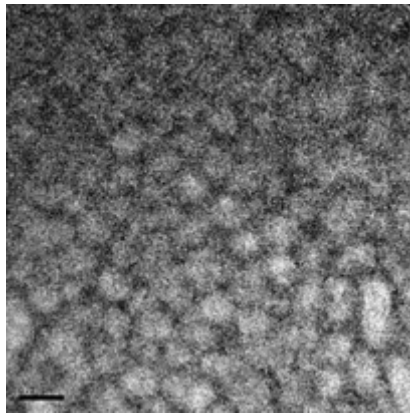
Thickness map



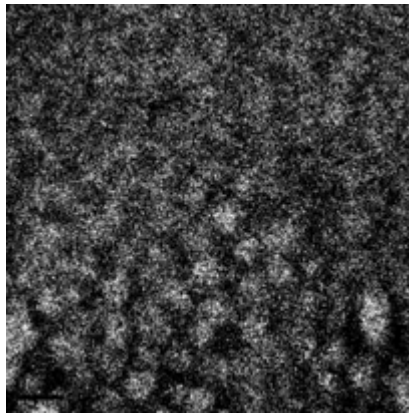
Cr L (574 eV)



Co L (779 eV)



Ni L (854 eV)

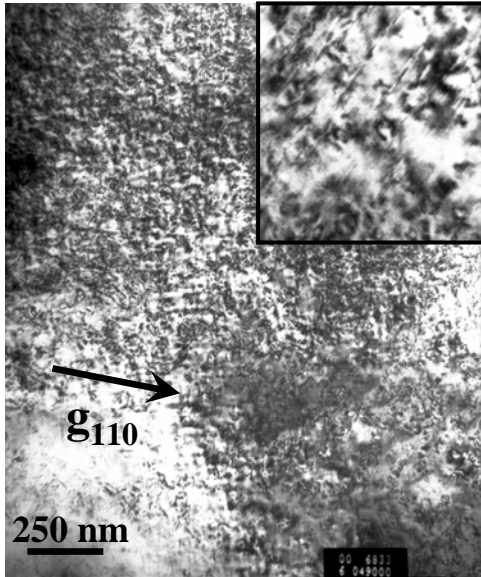


Al L (73 eV)

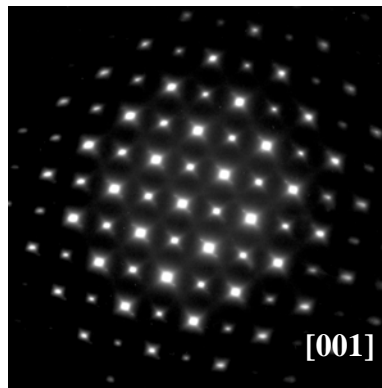
- The γ' precipitates are rich in Ni and Al while the matrix is rich in Cr and Co.

TEM observations of the β grains

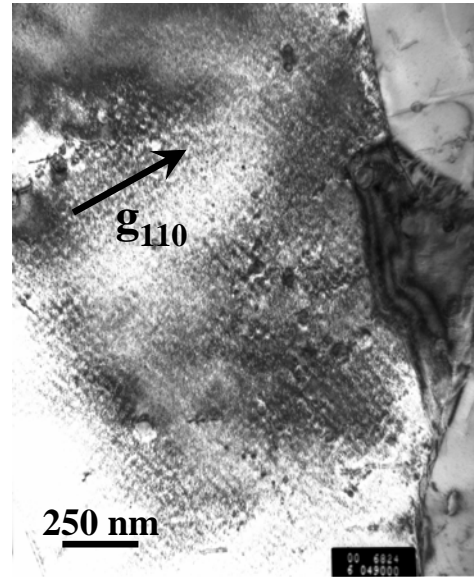
As-received



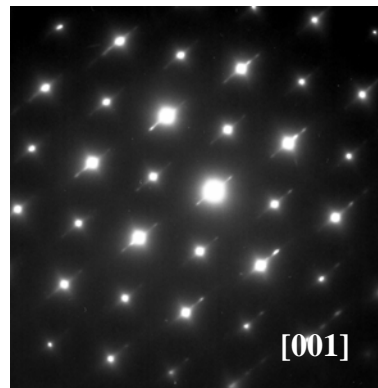
-Mottled-



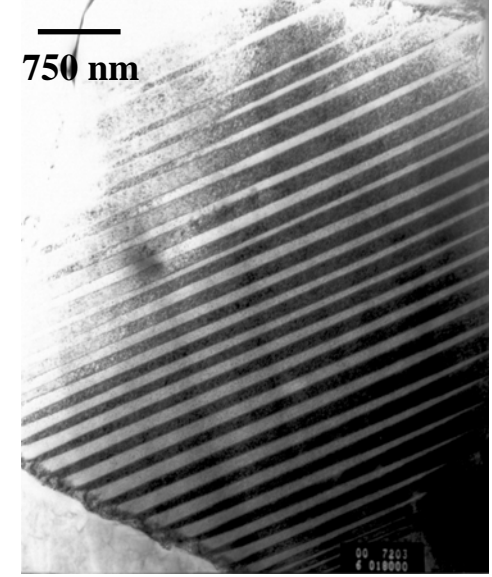
ELTB



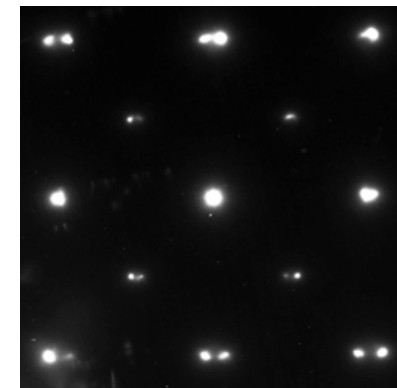
-Tweed-



100 hrs @ 1100°C



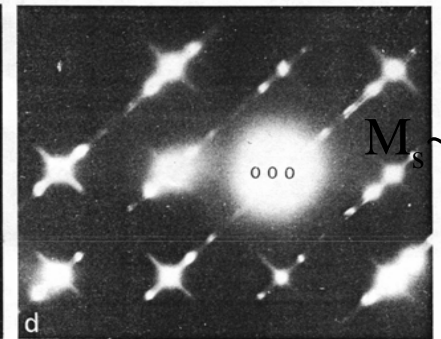
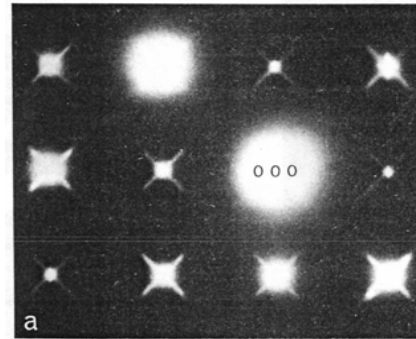
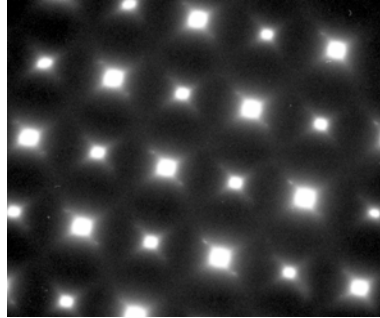
-Lath-



Do β -grains contain martensite?

$M_s \ll RT$

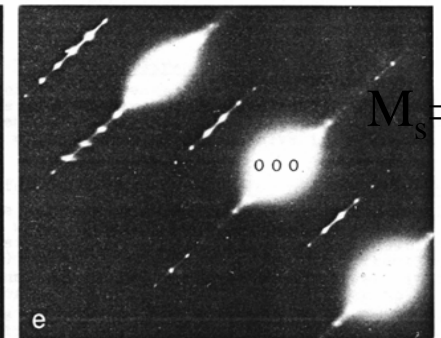
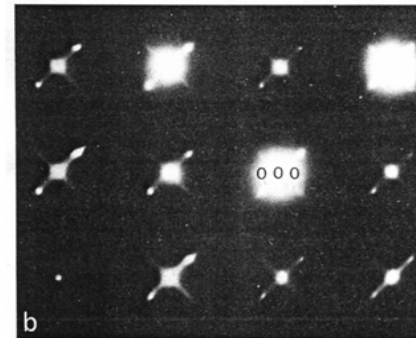
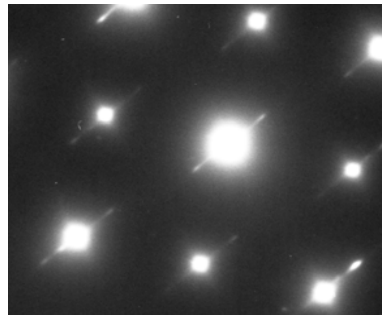
As-received



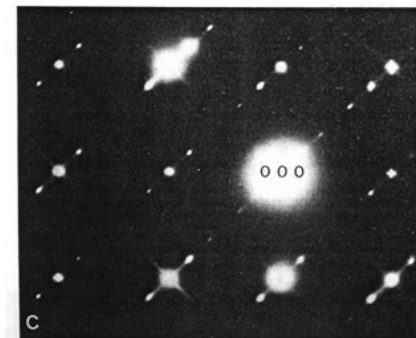
$M_s \sim T$

ELTB

$M_s < RT$

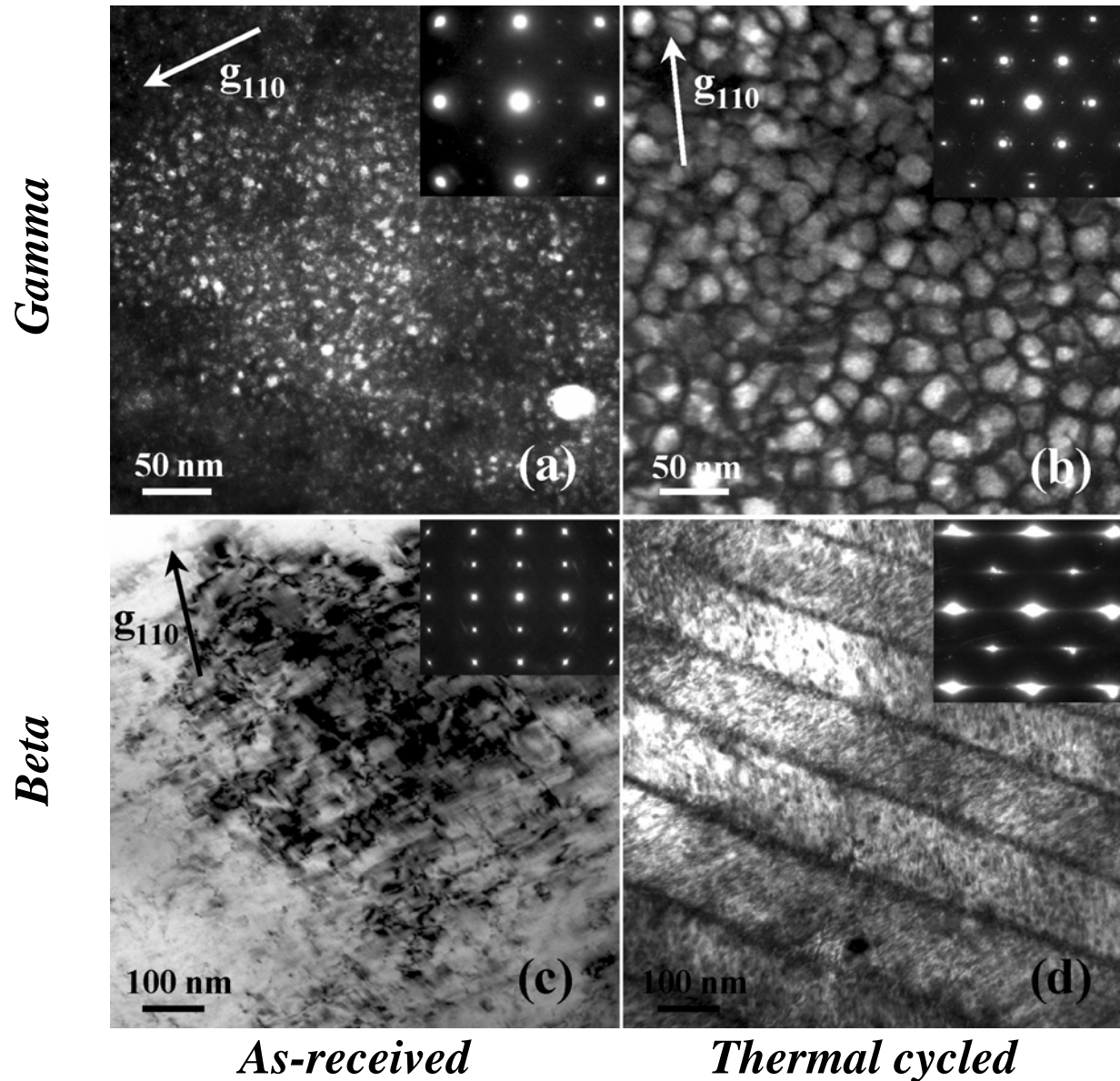


$M_s = T$

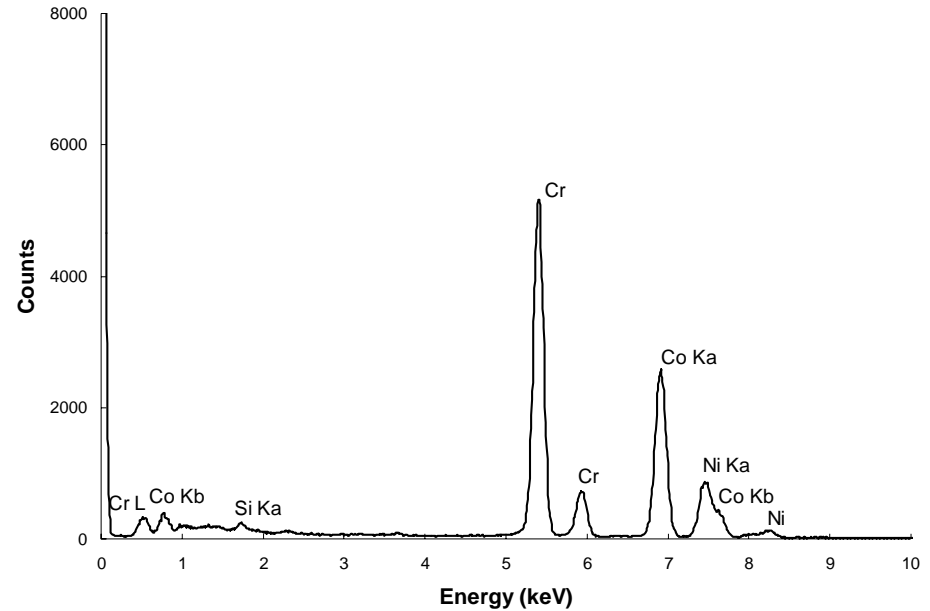
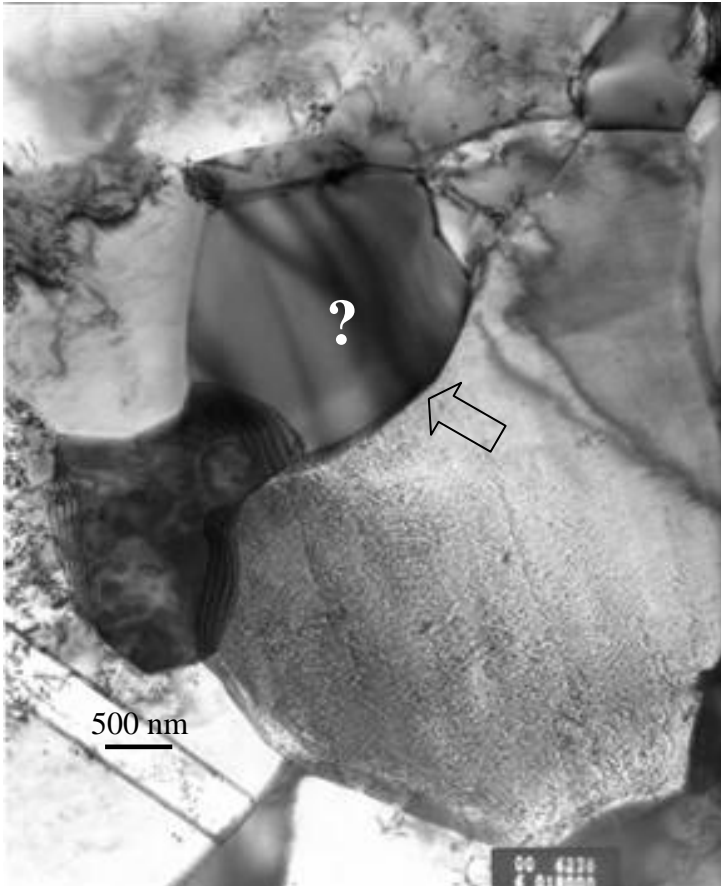


After Reynaud
Scripta (1977)

Microstructural evolution of NiCoCrAlY

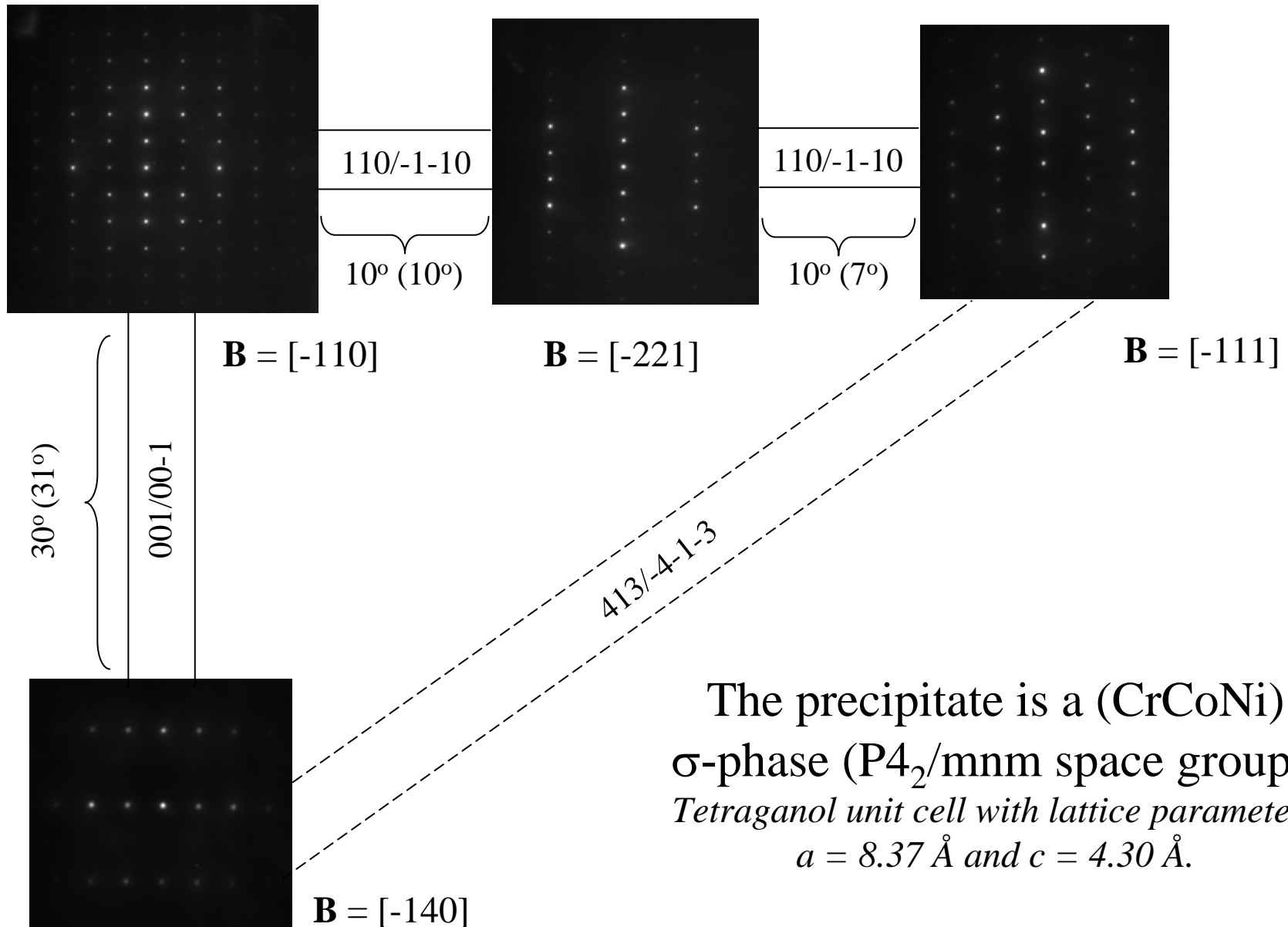


Precipitates found in an ELTB



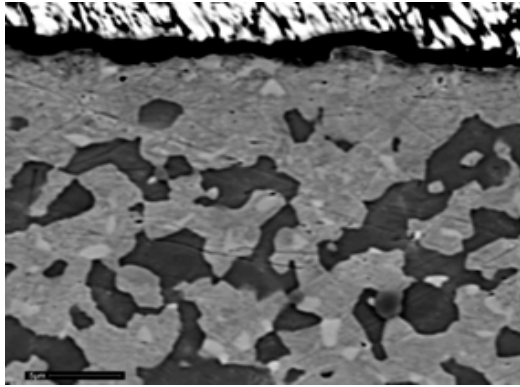
- Cr-rich intergranular precipitates widely dispersed in the ELTB specimen but not observed in the as-received samples.
- Composition is 55.5 at% Cr, 32.1 % Co, 11.0 % Ni and 1.4 % Si.

Crystal structure of Cr-rich precipitate

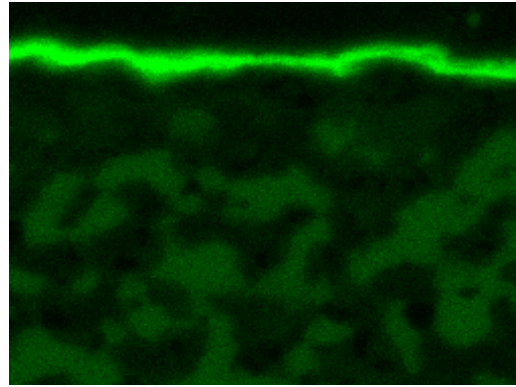


Elemental maps of the σ -precipitates

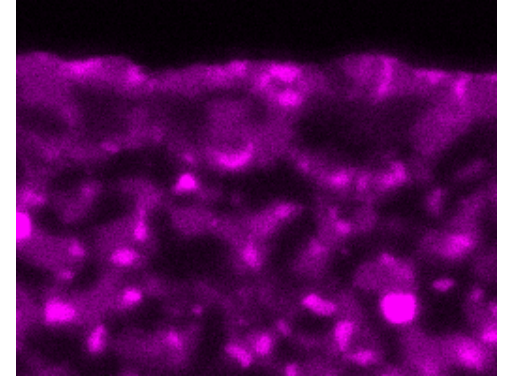
Mendis



Backscattered image

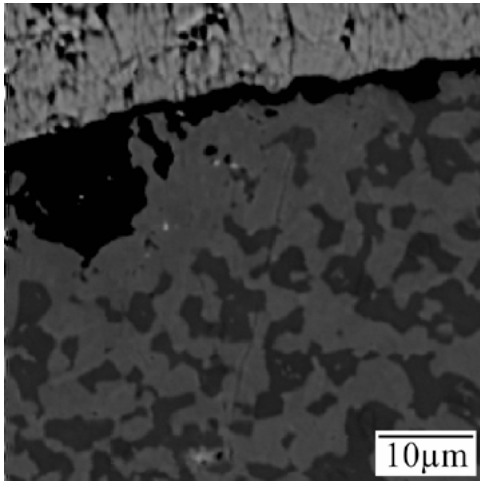


Al map

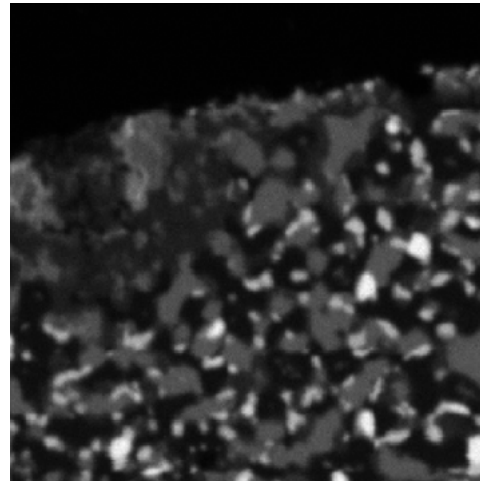


Cr map

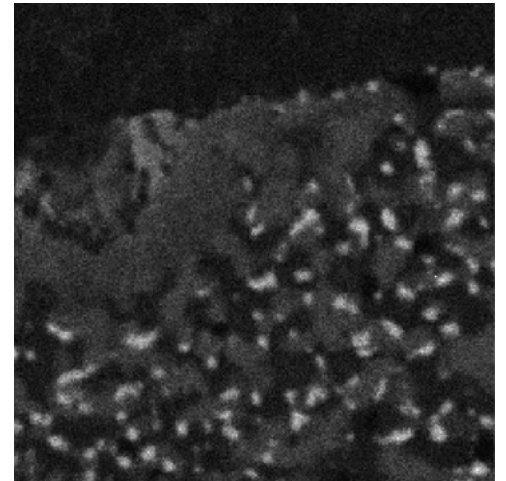
Tryon



Backscattered image



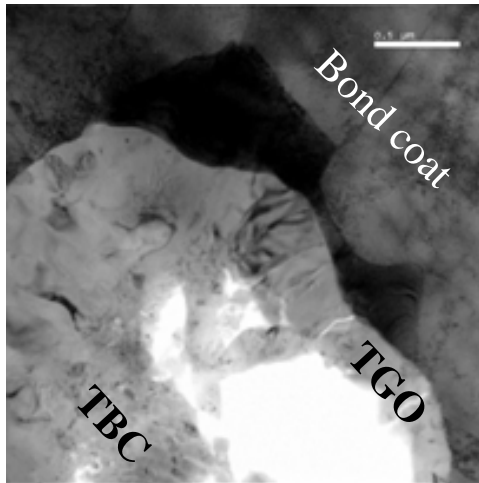
Cr map



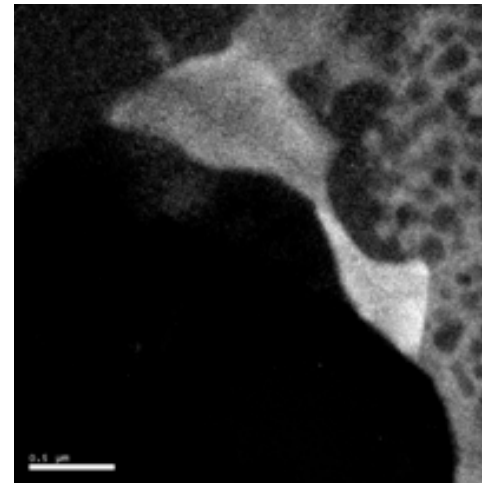
Si map

Potential impact of σ -phase ...

- Notoriously brittle but bond coat is not a load carrying structure.
- Appears to trap Si, which would mitigate its effect.
- Is observed at the TGO interface and may affect adhesion.



Elastic image



Cr L (574 eV)

- Note: only observed in ELTB;
not as-received or after 100hrs at 1100C!

Predicting phase stability...

Achar, Munoz, Arroyo, Singheiser, Quadackers, Modeling of phase equilibria in MCrAlY coating systems, Surface and Coating Tech (2004)

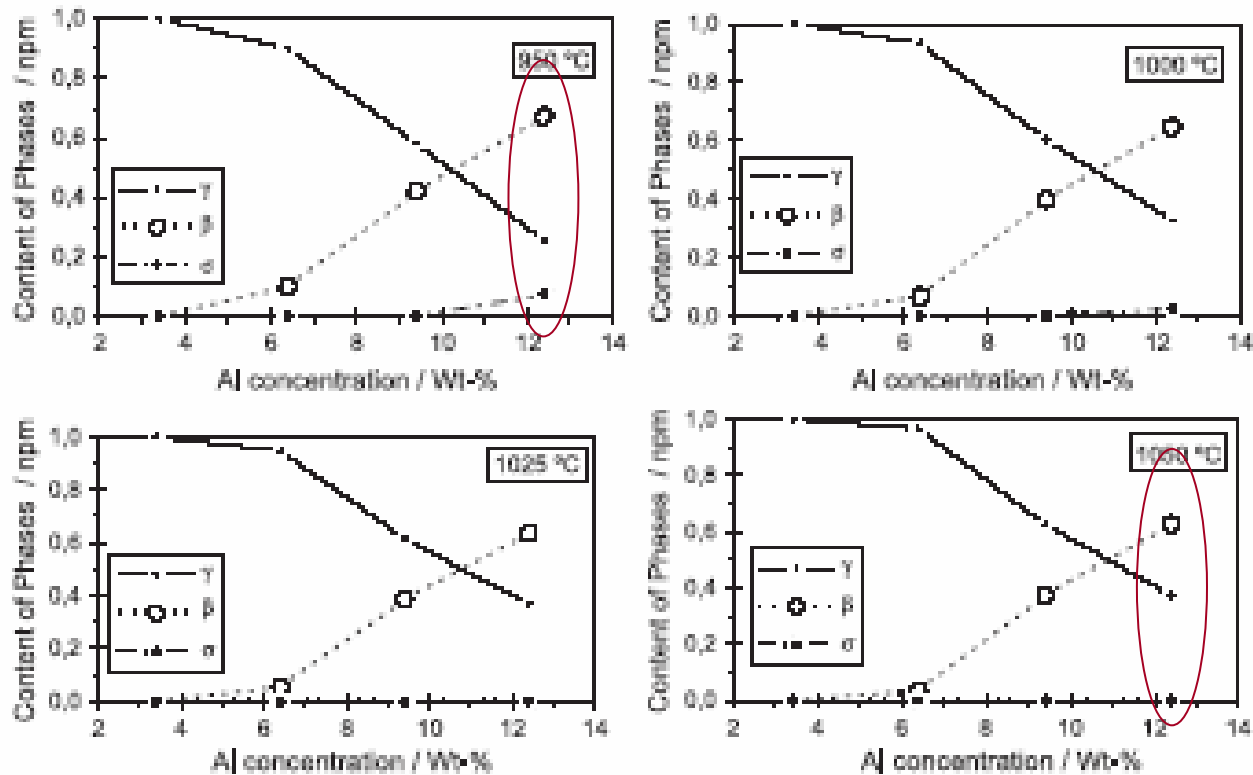
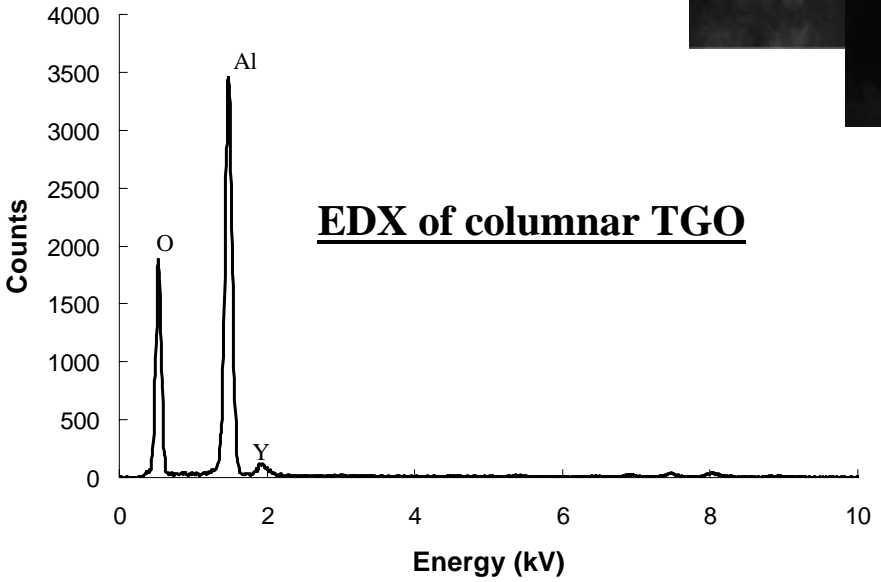
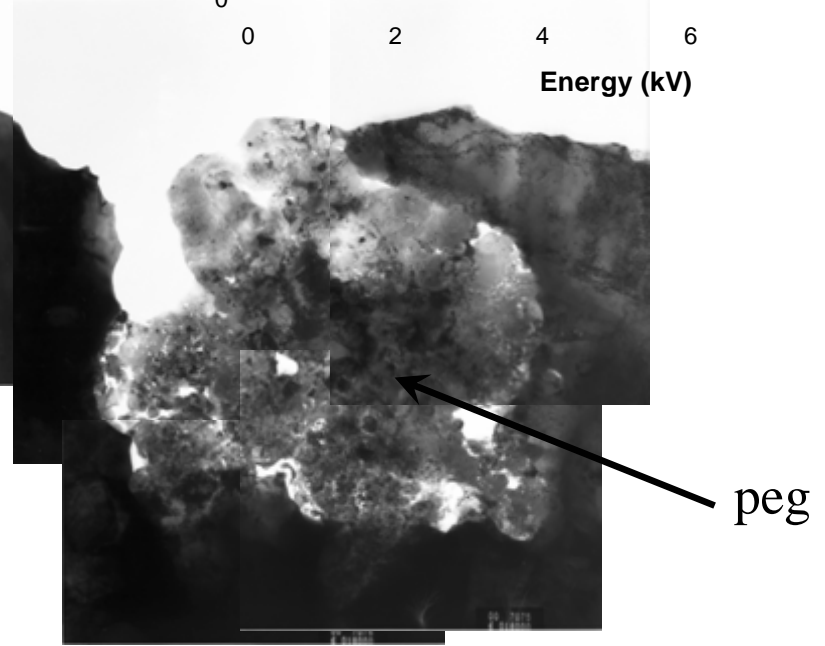
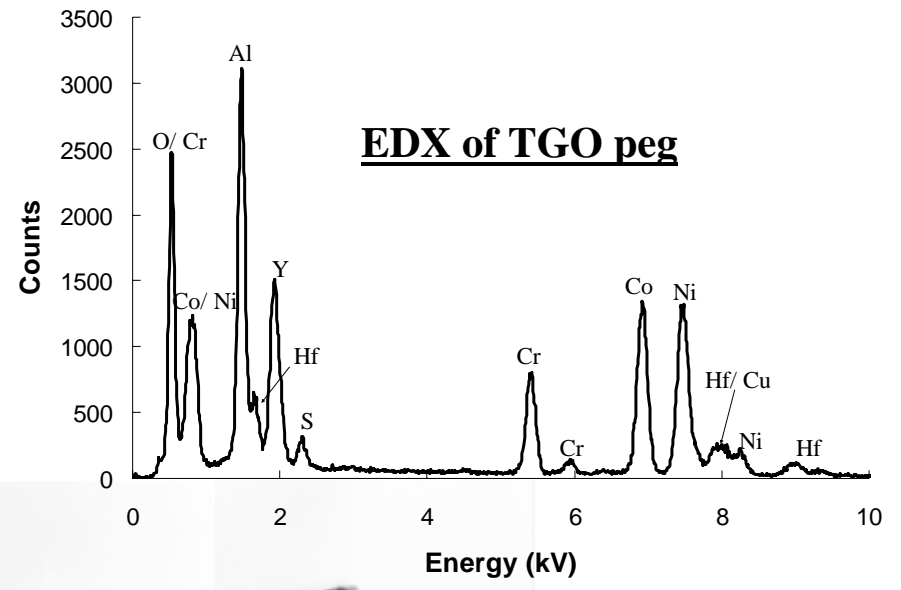
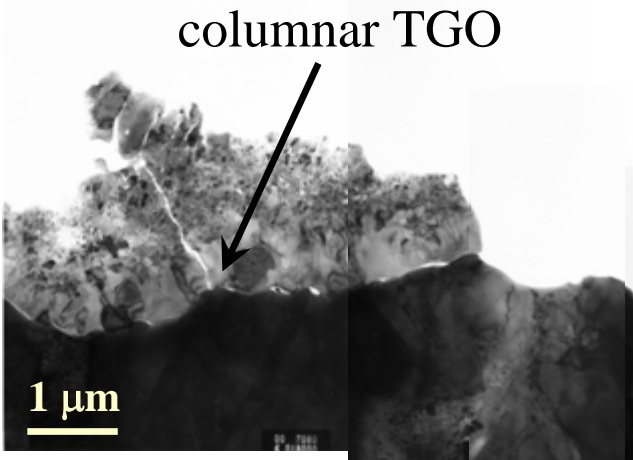


Fig. 7. Effect of Al content on calculated phase equilibria in quaternary Ni-20Cr-20Co-xAl coating alloys at different temperatures.

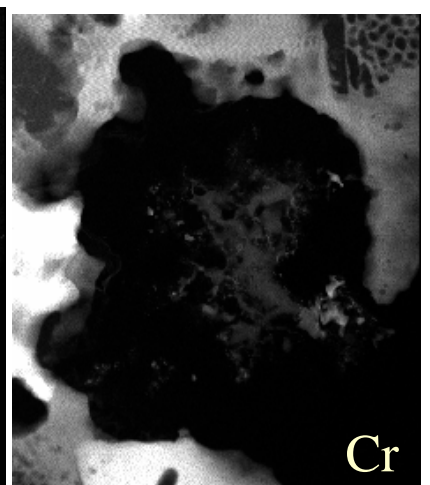
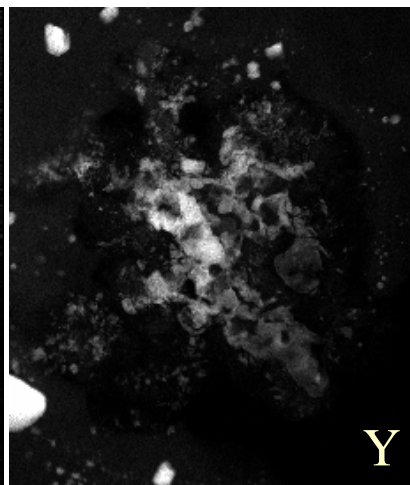
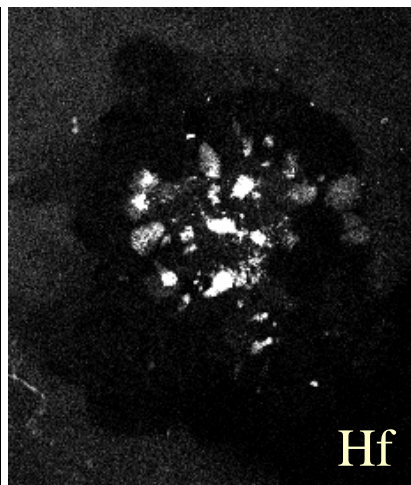
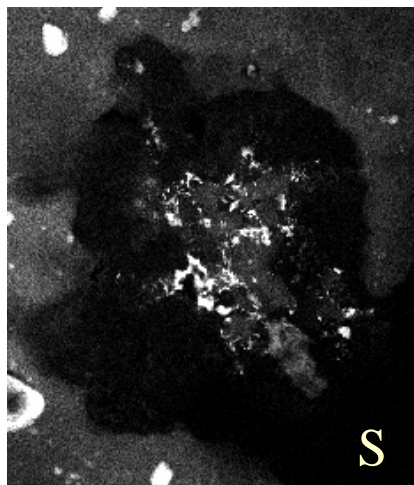
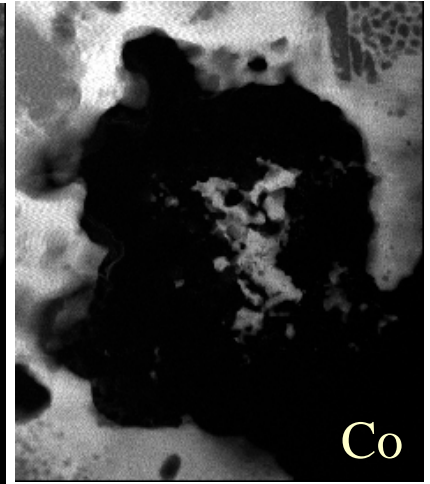
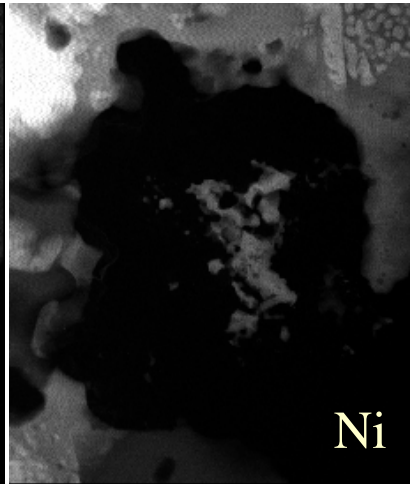
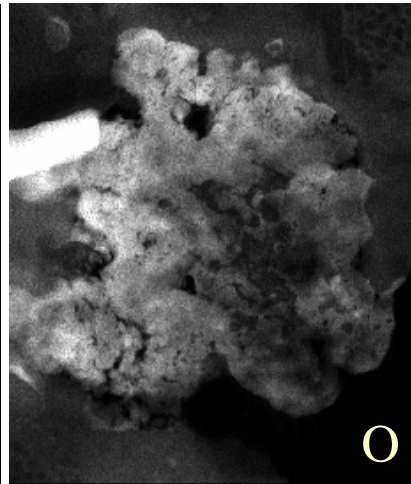
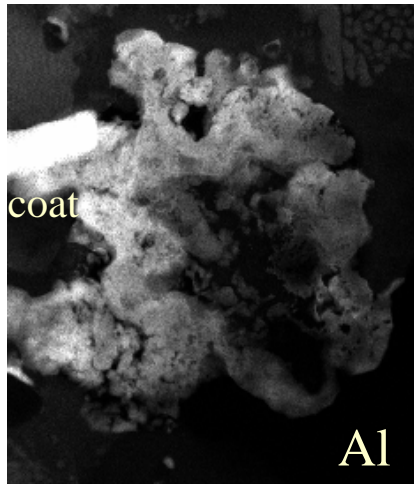
TGO and PEG Chemistry



The peg contains a large number of elements including sulfur, although the neighboring columnar TGO is nearly pure Al_2O_3 .

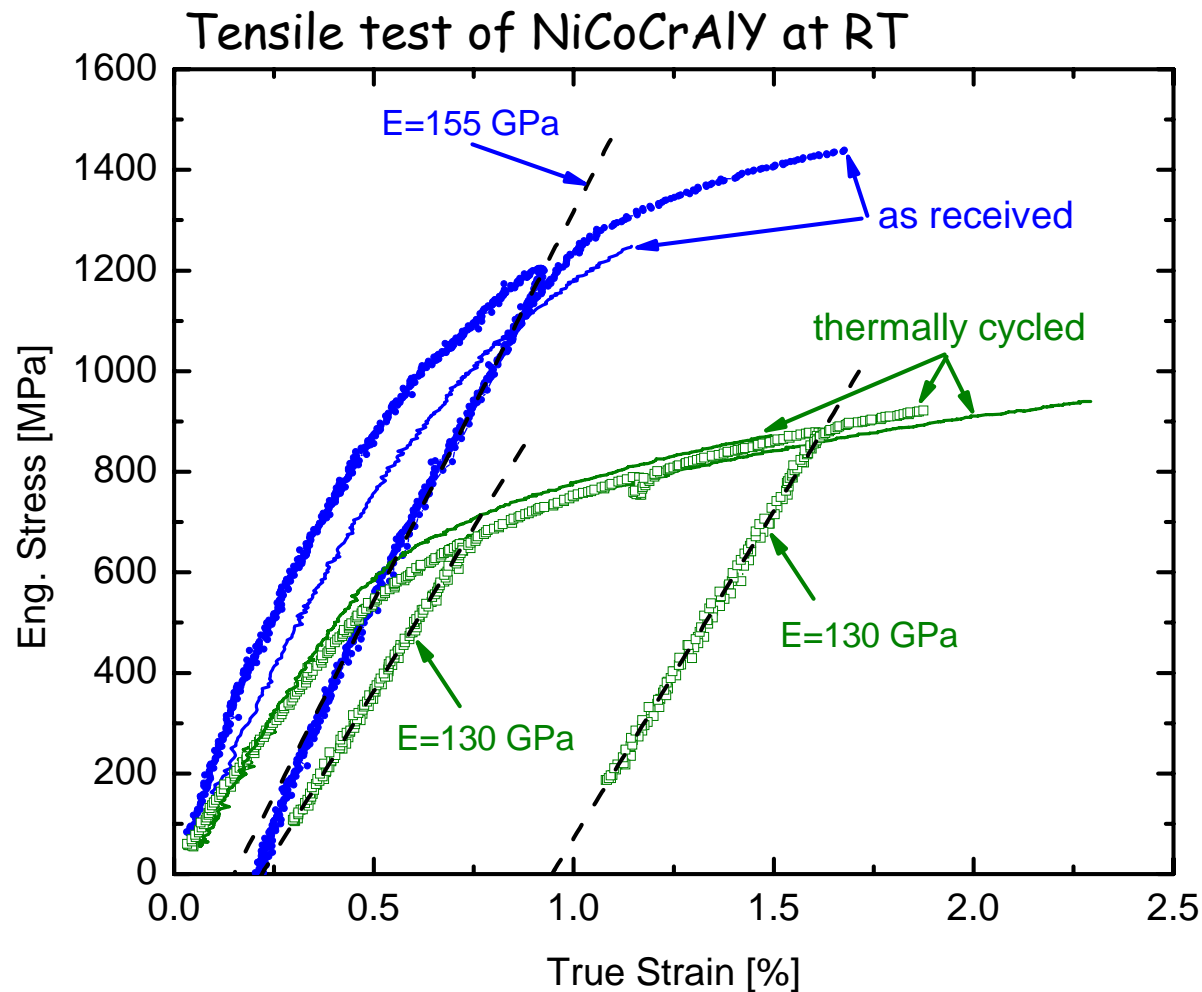
STEM shows S in pegs but not the TGO

Bond coat



Mechanical behavior of P&W's
NiCoCrAlY(Hf,Si) bond coat

RT strength of NiCoCrAlY

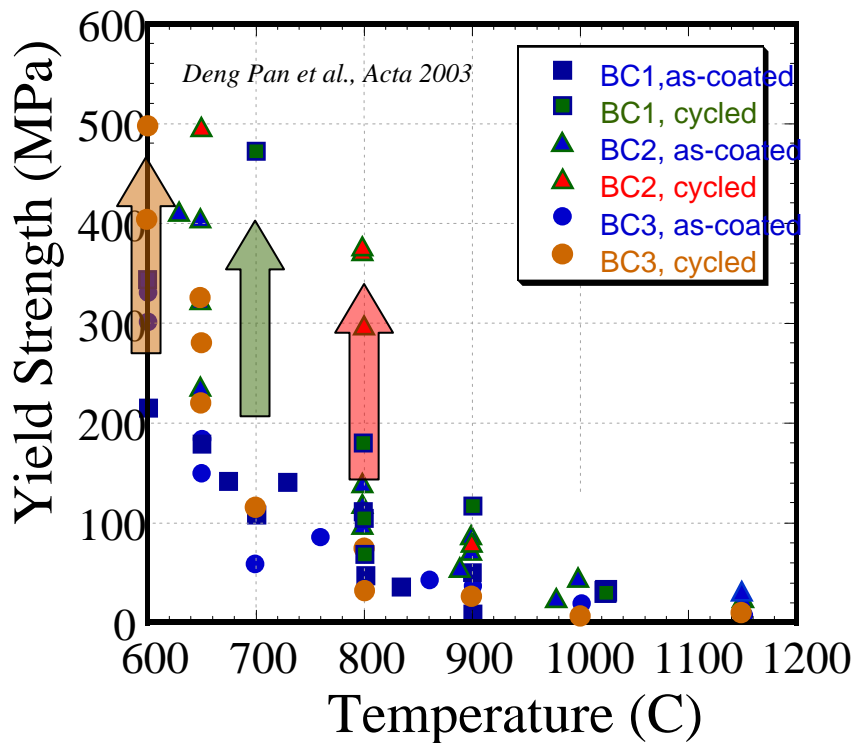


1.4 GPa
with RT
ductility!

Effect of thermal cycling

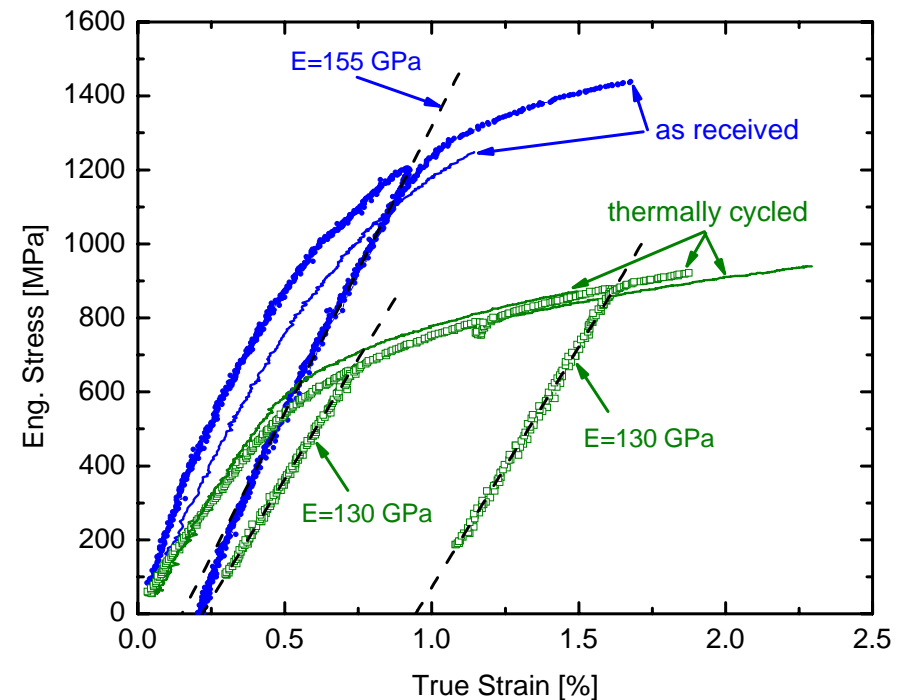
Diffusion alumine

- strength increases

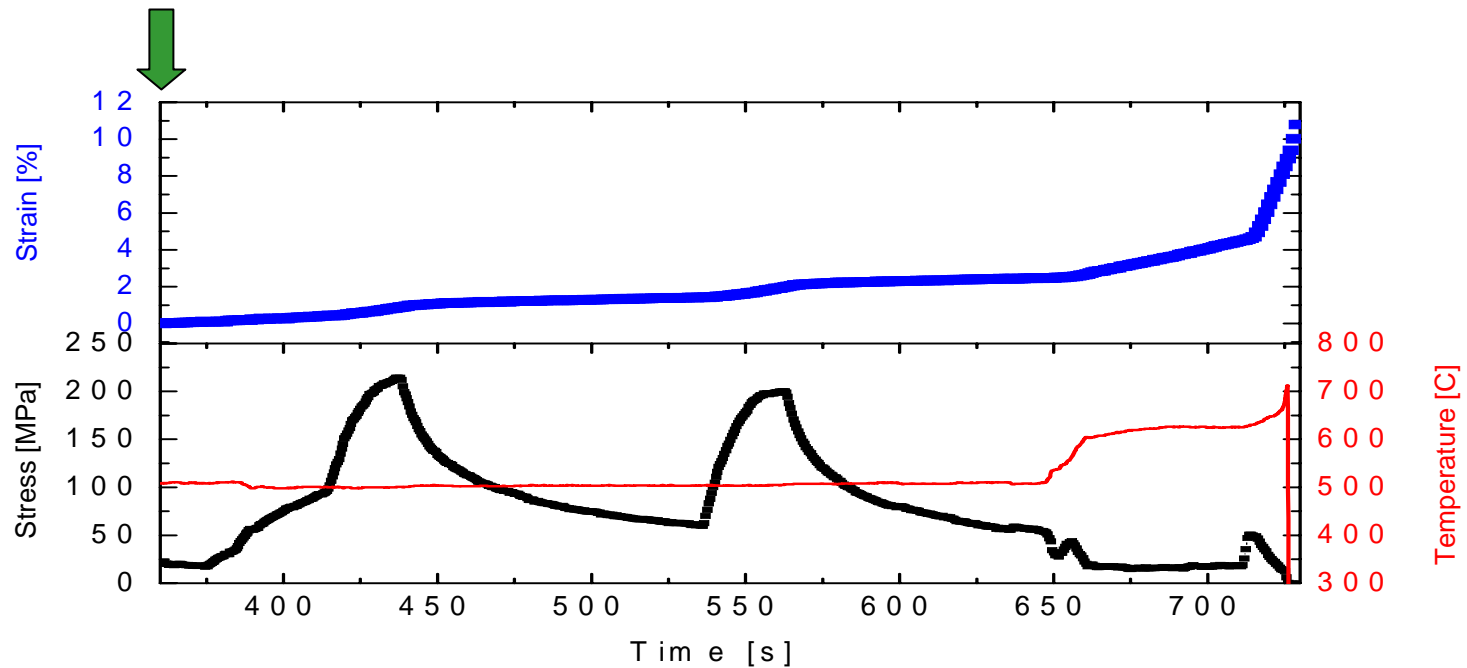
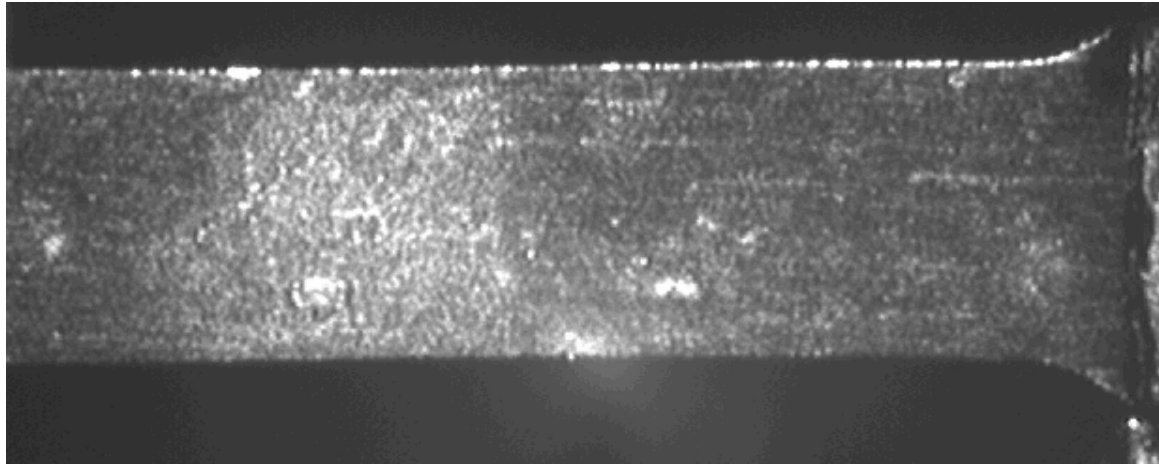


NiCoCrAlY

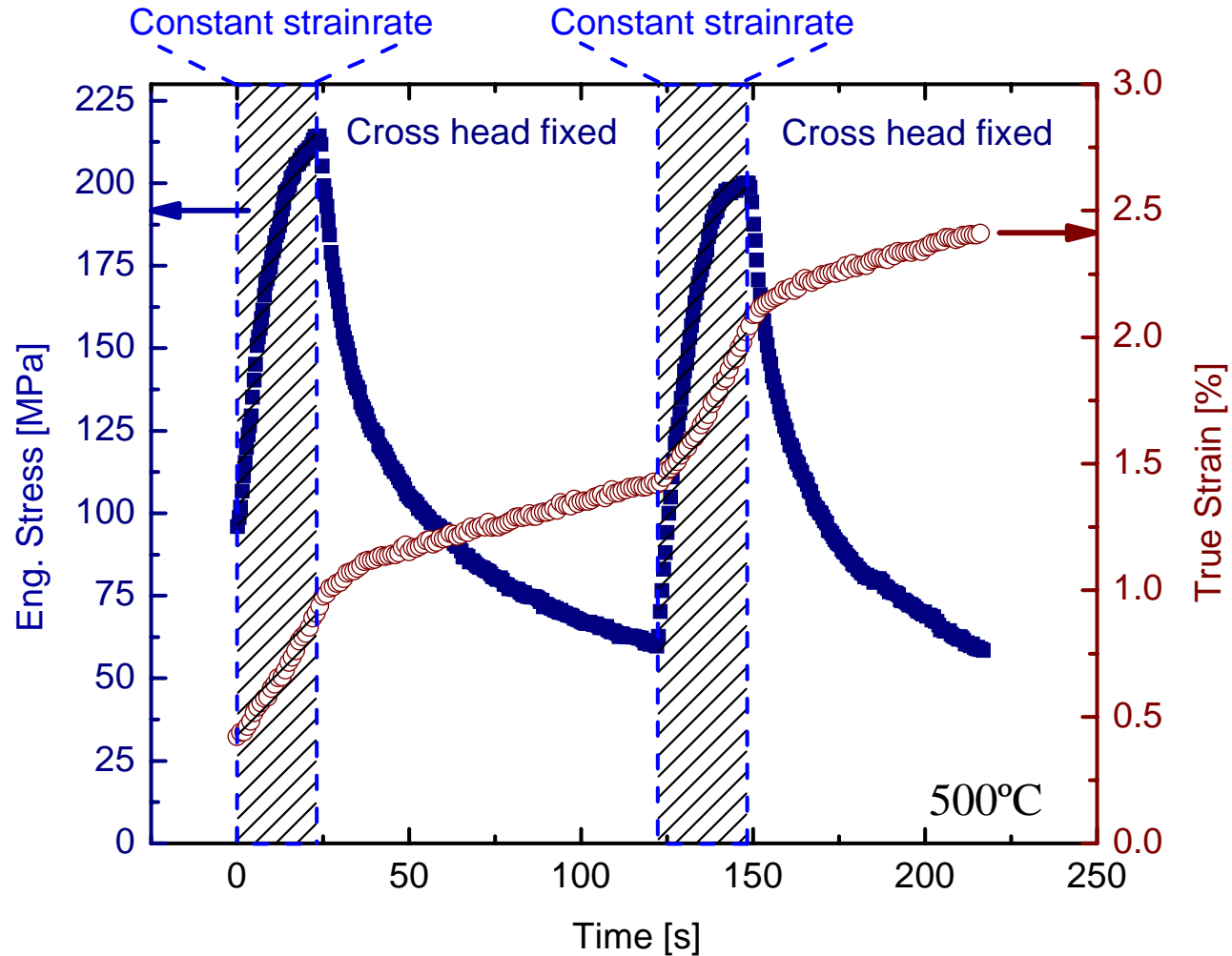
- strength decreases



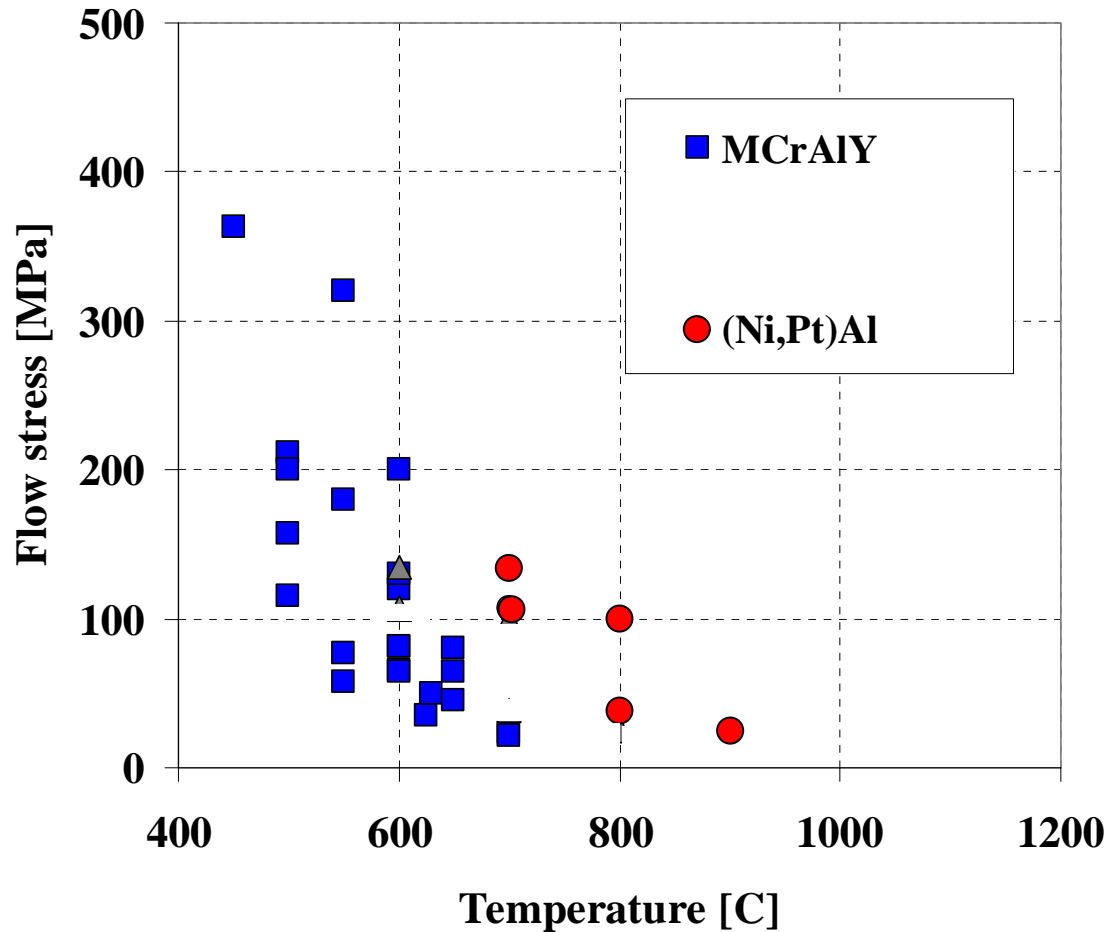
High temperature deformation:



High temperature deformation:

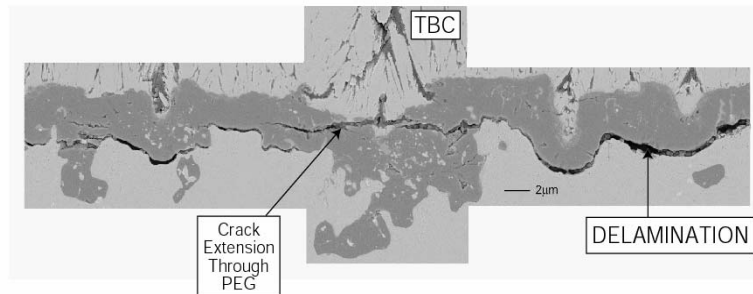
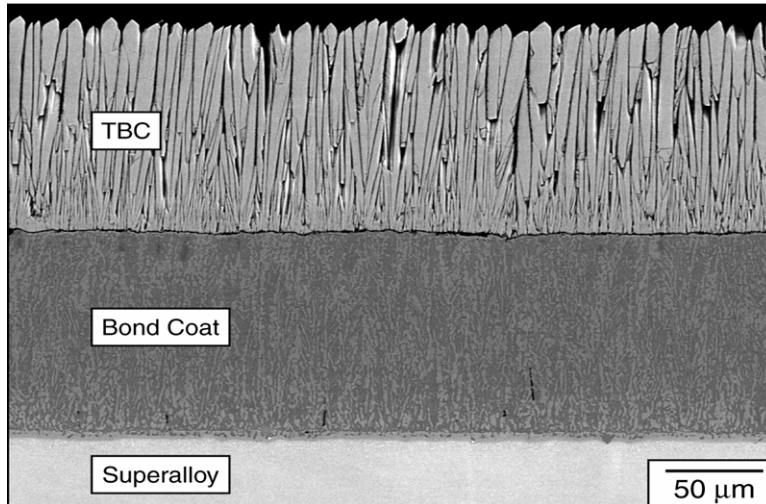


Comparison of high T strength:



Failure of NiCoCrAlY TBC systems

e.g. NiCoCrAlY bond coat systems



Salient observations:

- No TGO ratcheting.
- Cracks occur below the TGO.
- Crack growth is mode-II and effected by interfacial energy and plasticity in the adjacent layers.
- Cracks must be initiated before they can grow.

Proposed failure mechanism map:

